COLD FRONT SEDIMENT RESUSPENSION, AGE, AND RESIDENCE TIMES OF SUSPENDED SEDIMENT USING $^{7}BE/^{210}PB_{XS}$ RATIO IN GALVESTON BAY

A Thesis

by

NICOLE MARI SCHMIDT

Submitted to the Office of Graduate and Professional Studies of
Texas A&M University
in partial fulfillment of the requirements for the degree of

MASTER OF SCIENCE

Chair of Committee,	Timothy Dellapenna
Committee Members,	Kyeong Park
	Jens Figlus
Head of Department,	Shari Yvon-Lewis

August 2021

Major Subject: Oceanography

ABSTRACT

Winds associated with the passage of meteorological fronts cause wave-induced sediment resuspension, especially in shallow estuaries such as Galveston Bay. With a warming climate, the intensity of all meteorological events is increasingly having greater impacts on ecosystems. To better understand the effects that the passage of meteorological fronts has on the resuspension of sediment, water samples were collected during frontal passages at two locations in Galveston Bay. One in the middle portion of the bay, and one closer to the mouth of the bay. Additionally, a Conductivity, Temperature, Depth (CTD) data logger with an Optical Backscatter (OBS) turbidity sensor was deployed in Trinity Bay. We found stronger frontal winds are attributed to higher total suspended sediment (TSS) due to more sediment being resuspended from the bottom. This may, at least in part, be a result of the bay sediment in the middle bay having a finer grain size than the sediment within the lower bay. Additionally, ebb tide has higher TSS concentrations when there is a north wind in the middle bay, resulting from the addition of tidal current coupled with wind waves and wind-driven current imparting greater shear stress to the seabed. By collecting precipitation, water samples in both the middle and lower bay, and measuring the ratio of beryllium-7/lead-210 excess ($^{7}Be/^{210}Pb_{xs}$) in these samples; we can quantify the residence times of TSS in middle and lower Galveston Bay. Based on two sampling events on 1/29/2020, the age of the sediment in the middle bay was 70 ± 10 days (sampled on 1/29/2020), and 51 ± 7.8 days (sampled on 2/21/2020), where the lower bay had older suspended sediments, with 105 ±

15 days-old particles and 66 ± 10 days-old particles, respectively. This indicates that there are longer residence times when the water is trapped within the bay. Our estimated residence time of suspended sediments (51-105 days) suggests the particle-bound contaminants adsorbed to suspended sediment may spend months suspended in the bay before exiting the bay or being accreted into the bay sediment column, increasing the exposure time of living organisms to various particle-bound contaminants.

ACKNOWLEDGEMENTS

I would like to thank my committee chair, Dr. Dellapenna, and my committee members, Dr. Figlus and Dr. Park, and my colleague Dr. Lin for their guidance and support throughout the course of this research.

Thanks also go to the many colleagues that assisted in data collection during these cold storms. I would like to thank my friends and the department faculty and staff for making my time at Texas A&M University a great experience.

Finally, thanks to my mother and father for their encouragement.

CONTRIBUTORS AND FUNDING SOURCES

Contributors

This work was supervised by a thesis committee chaired by Associate Professor Timothy M. Dellapenna of the Department of Oceanography and Marine and Coastal Environmental Science.

Sample collecting was completed by the student along with undergraduate volunteers including Gregory Grimm, Ryland Lewis, Ryan Gage and Oscar Cavazos. All in-lab processing work conducted for the thesis was completed by the student independently, with assistance from Timothy Dellapenna, Peng Lin, and Josh Alarcon.

Funding Sources

This work was also made possible in part by National Oceanic and Atmospheric Administration (NOAA) and the Texas General Land Office Texas Coastal Management Program under Grant Number NA18NOS4190153. The contents of this thesis are solely the responsibility of the author and do not necessarily represent the official views of the NOAA or the Texas General Land Office.

NOMENCLATURE

CTD	Conductivity, Temperature, and Depth Sensor
MSL	Mean Sea Level
NOAA	National Oceanic and Atmospheric Administration
NWS	National Weather Service
OCSB	Ocean and Coastal Studies Building
OBS	Optical Back Scatter Sensor
TAMUG	Texas A&M University at Galveston
TCYC	Texas Corinthians Yacht Club
TSS	Total Suspended Sediment
TWBD	Texas Water Development Board

TABLE OF CONTENTS

Page

LIST OF FIGURES

Page

LIST OF TABLES

Page

1. INTRODUCTION

Sediment remobilization/resuspension plays a role in many estuarine processes; especially the cycling of nutrients and pollutants in and out of an estuary (Baskaran & Santschi, 1993). Point source and nonpoint source discharges of pollutants (e.g., trace metals and hydrocarbons) can have significant environmental impacts in an estuary (e.g., Dellapenna et al., 2006, 2020). These constituents can be stored in the sediment during periods of sediment deposition and are resuspended during wind-induced wave resuspension, in addition to any other resuspension events (Dellapenna et al., 2006). Particle reactive contaminants generally move slowly through an estuarine system, transported through the innumerous cycles of deposition and resuspension during various hydrological stages (Saari et al., 2010). Wind-induced currents and wave resuspension are important sources of energy for sediment transport within an ecosystem and can be dominant in shallow, microtidal estuaries, affecting a large portion, if not all of the water column (Booth et al., 2000).

High concentrations of total suspended sediment are most often associated with meteorologically driven events, especially winter cold fronts in the Northern Gulf of Mexico estuaries (Perez et al., 2000). Sediment resuspension associated with strong cold fronts can reintroduce trace elements and pollutants back into the water column, thus increasing the time that these particles are in the water column and adsorbed to sediments (Olsen et al., 1986). Contaminant discharge into a coastal system frequently occurs during storm events, especially if there is heavy precipitation (Du et al., 2020). Water bodies can be heavily impacted by pollution/contaminants from industrial activity,

etc. (e.g. heavy metals) (Saari et al., 2010). Once radionuclides adsorb to sediment particles, they are strongly and nearly irreversibly bound to these particles, making it possible to study the movement and obtain the age of suspended sediment (Taylor et al., 2013). The measurement of ^{7}Be and $^{210}Pb_{xs}$ activity in sediment quantifies the time that the particle surfaces sorbed the isotopes from the water column, which occurs when the particle becomes suspended in the water column (Matisoff et al., 2005). The ratio of ^{7}Be /$^{210}Pb_{xs}$ can be used to quantify the proportion of resuspended bottom material in the water column, with higher values indicating younger samples due to the short half-life (53 d) of ^{7}Be versus the longer half-life (22.3 y) of ^{210}Pb (Olsen et al., 1989). Sediment that has been recently labeled by radionuclides in the water were shown to display a similar ^{7}Be /$^{210}Pb_{xs}$ activity ratio to the rainfall event (Evrard et al., 2016).

The purpose of this study is to understand the relationship between cold fronts and sediment resuspension. Most meteorologically driven sediment resuspension occurs during the passage of northern cold fronts which mainly occur during winter months (Henry 1979, Hardy and Henderson, 2003). The following research questions are made to understand sediment transport during cold fronts: Will the age of sediment flow from upstream to downstream towards the mouth of the bay, and thus will the ratio of $^{7}Be/^{210}Pb_{xs}$ decrease? It has been previously observed that rainfall affects isotope activity of ^{7}Be and ^{210}Pb due to fallout patterns, in what way does it increase or decrease activity in Galveston Bay (Baskaran et al., 1993)? What are the main drivers affecting TSS resuspension during cold fronts (i.e. wind speed and tide)? Is TSS higher in the middle bay versus the lower bay?

It is hypothesized that the age of the sediment should be younger in mid Galveston Bay and older towards the mouth of Galveston Bay (lower-bay site), whereas the $^{7}Be/^{210}Pb_{xs}$ ratio and percent of new sediment should decrease towards the mouth of Galveston Bay. In regard to activities, it is hypothesized rainfall is directly related to the activity of both isotopes due to their fallout characteristics. Lastly, it is hypothesized that TSS during cold fronts with strong wind speeds (>6 ms^{-1}), will result in higher TSS than for wind speeds less than 6 ms^{-1}. As sediment moves through an estuary, the age of sediment should increase as its residence time within the estuary increases as the sediment is transported through the estuary, towards the ocean. With the abundance of clay-dominated mud in the middle bay and coarser mud (e.g., higher silt content, with sand) in the lower bay, total suspended sediment (TSS) concentrations will be higher in middle Galveston Bay versus closer to the mouth, allowing for deposition of coarser mud to occur at a faster rate than finer muds.

The combination of wind speed and precipitation that accompanies cold fronts will allow the measurement of activities of both ^{7}Be and ^{210}Pb needed to estimate the age of precipitation and suspended sediment. By collecting rainwater samples, and two separate water samples (e.g., middle and lower bay) during sampling events during each cold front event and measuring the ratio of $^{7}Be/^{210}Pb_{xs}$ in these samples; it is possible to quantify the residence times of suspended sediment in middle and lower Galveston Bay. Using the two samples from the middle and lower bay to measure suspended sediment within the water column during cold fronts, along with instrumental data collection may permit quantification of sediment resuspension during the passage of a frontal system.

Understanding physical processes, such as sediment resuspension and residence times, allows for proper management strategies to be developed to ensure a stable and productive ecosystem in the estuary (Walker and Hammack., 2000).

2. BACKGROUND

2.1. Galveston Bay Characteristics

Galveston Bay is a shallow, microtidal estuary and is the second largest estuarine system in Texas with a surface area of approximately 1360 km^2 (Dellapenna et al., 2006). The average depth of the bay is 2.1 m and contains a ship channel with dimensions of 150 m in width and 10-15 m deep, oriented along the main axis of the bay (50 km long) (Du & Park, 2019). The exchange of tidal water flows through Bolivar Roads, which is the tidal inlet between Bolivar Peninsula and Galveston Island. An additional inlet exists 47 km to the west and provides gulf flow to Christmas Bay and the western half of West Galveston Bay. Average water residence time within Galveston Bay is approximately 40 days (Solis and Powell, 1999). Trinity Bay comprises the northeastern portion of Galveston Bay (Fig. 1), has depths generally ranging between 3-4 m (Dellapenna et al., 2006) and the Trinity River flows into the head northeastern end of the bay, The Trinity River accounts for approximately 90% of the freshwater input and is the largest sediment source into Galveston Bay (SAGE, 2002, USGS, 2005). Another significant sediment load within the bay is the ongoing maintenance of the Houston Ship Channel. In waters deeper than 1.5 m, Trinity Bay bottom sediment is mud dominated (approx. 40% of total bay area) (Dellapenna et al., 2006). Mud is the dominant sediment composition of the majority of the Galveston Bay system (Fig. 1).

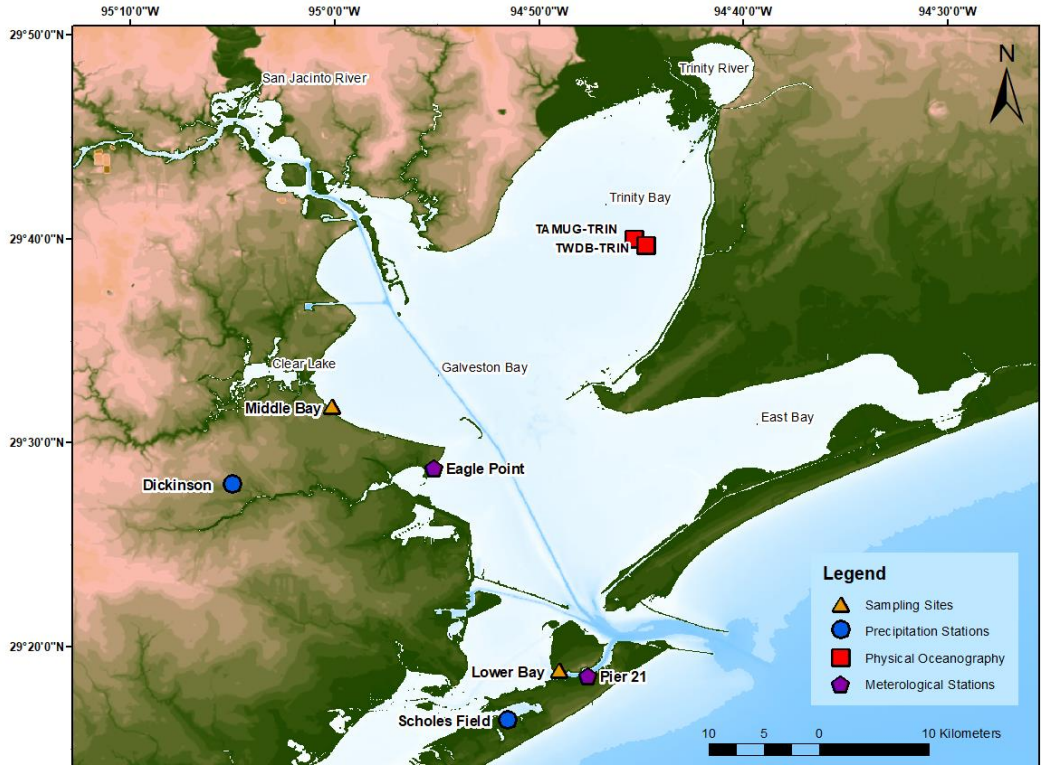

Figure 1 Map of study area and stations. meteorological stations (pentagon), precipitation stations (circle), suspended sediment and precipitation sampling sites (triangle), and physical oceanography sites (square).

The watershed of Galveston Bay contains both metropolitan Houston as well as the Clear Lake-Texas City-Galveston area and the Port of Houston. Houston, Texas, is the fifth-largest metropolitan area (population of 7 million), is the fourth-largest city in the US, and hosts the second-largest petrochemical complex in the world (Morse et al., 1993; Santschi et al., 2001). The Port of Houston is the second-largest seaport in the U.S. in terms of total shipping tonnage (Chambers et al., 2018) and services the 80 km long Houston Ship Channel, which extends up the axis of Galveston Bay from Bolivar Roads at its entrance to the San Jacinto Estuary and Buffalo Bayou. Further south of

Houston is the Clear Lake-Texas City-Galveston area which is also heavily industrialized, dominated by petroleum, petrochemical, and chemical industries as well as shipyards in Galveston. Collectively, the shores and watershed of Galveston Bay host nearly 50% of total US chemical production and oil refineries (Santschi et al., 2001). Galveston Bay also receives a significant amount of wastewater discharges for the state from surrounding facilities.

2.2. Cold Fronts

In Galveston Bay, there are on average, 20-30 cold fronts a year that pass, whereas hurricanes and tropical storms impact the bay on average once every 1.5 years, collectively (Byrne, 1975, Roberts et al., 1987, Walker and Hammack, 2000). Overall, cold fronts occur generally between October through April and have fairly consistent characteristics (Roberts et al., 1987, Walker and Hammack, 2000). The cold fronts begin as a passage defined by a shift from southerly to northly wind direction that propagates in a clockwise direction (Perez et al., 2000). Cold fronts are thought to have larger impacts on the coastal environment than tropical storms due to higher frequency along with wind shifts (Roberts et al., 1987, Moeller et al., 1993, Pepper et al., 1999). This is due to the creation of waves caused by the wind shifts that transports fluid mud from one area to another (Kemp, 1986). There is a natural variability of wind including the orientation, propagation direction, and strength of winds produced during cold front events that dictates the effect of suspended sediment movement within an estuary (Moeller et al., 1993). Wind direction and speed have been shown to be the primary factors controlling sediment resuspension, sediment transport and circulation (Walker

and Hammack, 2000). Dellapenna et al. (2006) estimated that the sediment resuspension that results from cold fronts has an annual equivalence of 200-270% of the suspended sediment load from Galveston Bay's fluvial source.

2.3. Sediment Resuspension

Galveston Bay provides nursing habitat for multiple valuable fisheries, including white and brown shrimp (Stunz et al., 2010) and provides approximately 14% of the US wild catch of oysters (Haby et al., 2009). A key process in shallow estuaries is the frequency of sediment resuspension. An increased amount of sediment resuspension and deposition in an estuary may cause smothering of benthic aquatic organisms and the clogging of water intakes (Winterwerp & VanKersteren, 2004).

Turbidity is a measure of the degree to which water loses its transparency (Hardenbergh, 1938) and is due to both the presence of suspended particles, including sediment, as well as phytoplankton, particulate organic matter, and other particulates (Biggs, 1970; MacIntyre & Cullen, 1996). Total suspended sediment (TSS) is the quantification of the mass of sediment that is suspended in the water column. TSS is characterized as being particles that settle too slowly to fall out of suspension during slack water (Sanford & Halka, 1993). Suspended sediment is derived from the erosion, or resuspension at the water-sediment interface and river input (Ha & Park, 2012). TSS concentrations can also vary widely depending upon riverine input, wind forcing, drainage basin size, depth, area of the bay, sediment composition, and tidal range (Perez et al., 2000). Based on findings in Walker and Hammack (2000) sediment resuspension and transport are maximized during the passage of winter storms over Louisiana

estuaries. Throughout a study performed in Fourleague Bay, Louisiana, northerly winds were found to have the greatest wind velocities; and wind direction played an important role in the transport of water and sediment (Perez et al., 2000). Additionally, Perez et al. (2000) found that total suspended sediment peaks were highly correlated to post-frontal winds. The residence time of suspended sediment is defined here as the average length of time during which the sediment resides within the bay as suspended sediment. The residence time of suspended sediment in the water column has been found to range from a few days in low-energy estuaries to several weeks in high-energy estuaries (Olsen et al., 1986).

2.4. Characteristics associated with cold fronts

Wind plays an important role in determining water level in many shallow-water, microtidal coastal plain estuaries, including Galveston Bay (Cox et al., 2002). Surface gravity waves are the primary mechanisms driving sediment resuspension in shallow, microtidal estuaries (Booth et al., 2000). During these winter storms, wind speed greater than 10 ms^{-1} causes the strongest sediment resuspension (Walker and Hammack, 2000). Cold fronts are accompanied by a high variability of wind speed and wind direction that largely affect TSS concentrations and fluxes (Perez et al., 2000). Booth et al. (2000) states that resuspension events are highest during fall, winter, and early spring due to frequent and intensive cold front events. In relation to cold fronts, winds above 10 ms^{-1} can cause resuspension of more than 80% of bottom sediments based on a study performed in Louisiana (Booth et al., 2000). Sanford and Halka (1993) stated that sediment is 2-4 times more erodible shortly after being deposited versus sediments that

were deposited for over a year. Cold fronts are important mechanisms for resuspending/remobilizing sediment in shallow estuaries, such as Galveston Bay (Carlin et al., 2016).

2.5. Isotopes

Short-lived radionuclides can be useful for studying seasonal particle dynamics under different flow regimes (Saari et al., 2010). Short half-lives, for example, 53 days for ^{7}Be and 24 days for ^{234}Th, and 23 years for ^{210}Pb, provide an advantage when considering recent events that cause sediment redistribution (Taylor et al., 2013).

^{7}Be is a cosmogenic radionuclide produced in both the stratosphere and troposphere as a result of cosmic ray spallation of nitrogen and oxygen (Brost et al., 1991). Following atmospheric fallout, ^{7}Be rapidly adsorbs to fine sediment particles (Taylor et al., 2013). ^{7}Be also serves as an indicator of recent sedimentation and transport of surface material on a catchment scale (Taylor et al., 2013). Many studies have demonstrated that deposition of ^{7}Be closely reflects rainfall volume, making it a useful tracer for studying events that relate to rainfall, such as cold fronts (Olsen et al., 1986; Baskaran & Santschi, 1993; Baskaran et al.,1993; Taylor et al., 2013; Evrard et al., 2016; Mabit & Blake, 2019). During cold front events when sediment resuspension is high, ^{7}Be within the bed sediment can be recycled back into the water column and interact with newly delivered ^{7}Be (Olsen et al., 1986).

^{210}Pb is a member of the ^{238}U decay chain. When ^{238}U decays in soils, it become ^{226}Ra and then decays into ^{222}Rn. Since radon is a noble gas, it emits from the land into the atmosphere where it decays to ^{210}Pb (atmospheric) (Baskaran et al., 1993). ^{210}Pb is

released from the atmosphere and delivered from the surface via wet and dry fallout. ^{210}Pb is called $^{210}Pb_{xs}$ once it has adsorbed to particles by the decay of its' parent isotope.

Fallout patterns of ^{7}Be and ^{210}Pb are tightly correlated leading to these nuclides being useful for dependent tracers (Baskaran et al., 1993). The similarities of ^{7}Be and ^{210}Pb as tracers include similar atmospheric deposition and strong adsorption to similar particles; meaning they do not preferentially adsorb to specific particle sizes or compositions. Therefore, using the activity ratio of these two particles is less variable than either isotope individually (Matisoff et al., 2005). Once radionuclides adsorb to sediment particles, they are strongly and nearly irreversibly bound to these particles, making it possible to study the movement and obtain the age of suspended sediment (Taylor et al., 2013). $^{210}Pb_{xs}$ and ^{7}Be activities in the water column (dissolved and particulate) have been found to vary with precipitation and river discharge (Sommerfield et al., 1999, Baskaran & Swarzenski, 2007). The measurement of ^{7}Be and $^{210}Pb_{xs}$ nuclide activity in sediment quantifies the time that the particles sorbed the isotopes from the water column (Matisoff et al., 2005). Sediment that has been recently labeled by radionuclides in the water were shown to display a similar ^{7}Be /$^{210}Pb_{xs}$ activity ratio to recent rainfall (Evrard et al., 2016). The ratio of ^{7}Be /$^{210}Pb_{xs}$ can also be used to quantify the proportion of resuspended bottom material in the water column (Olsen et al., 1989). Baskaran and Santschi (1993) found that concentrations of ^{7}Be are quickly diluted into coastal waters and sediment in 1-2 days following rainfall events.

3. DATA AND PROCESSING

3.1. CTD Deployment

An RBR CTD (conductivity, temperature, and depth sensor) with two Seapoint optical back-scatter sensors (turbidity) was mounted to a homemade frame (pod) built for deployment in Trinity Bay from January 27, 2020 to February 27, 2020. One sensor was mounted 50 cm above the bed, and the other sensor was mounted 150 cm above the bed. The reasoning for the sensor placements is that the sensor at 50 cm would likely be within the threshold where sediment becomes resuspended during wind waves. The sensor placed at 150 cm is assumed to be above this threshold. Unfortunately, the only sensor that collected data was the one placed at 50 cm from the bed, therefore making it not possible to compare the two sensor data recordings. The CTD was set to measure every 6 hours so that the battery life would last for over a month of deployment. Three 45 kg dumbbell weights were mounted at the base of the pod to keep it from moving during strong cold front events. Water was collected during deployment and upon retrieval to calibrate the sensors for TSS. The Trinity Bay TAMUG-TRIN Station was chosen for the CTD because the area is known to generally be characterized by a mud dominated-bottom (Dellapenna et al., 2006). For the TAMUG-TRIN station an abandoned production platform was selected and the instrument pod was placed between two legs of the platform to ensure that it would not be entangled by shrimp nets or oyster dredges. It is important to note that, based on the instrument results, it is assumed that significant biofouling of the OBS sensor began on February 8th, 2020. The OBS sensor was impacted by biofouling more detrimentally than the conductivity and temperature

sensor because this sensor relies on light transmission through the water column, whereas the other parameters on the CTD do not. Biofouling could have covered parts of the OBS sensor, keeping it from accurately recording TSS. From looking at the data (Fig. 10), it appears that both temperature and conductivity do not drastically differentiate throughout the deployment unlike the OBS sensor.

3.2. Turbidity Sensor Calibration

TSS concentrations were determined from the OBS sensor attached to the CTD during the TRIN pod deployment. Concentrations were calculated using the linear equation formula (y = 0.0018x + 0.08). The calibration of the CTD Seapoint turbidity sensors was performed in the lab using sediment and water collected on site during deployment of the CTD in Trinity Bay (Fig. 3).

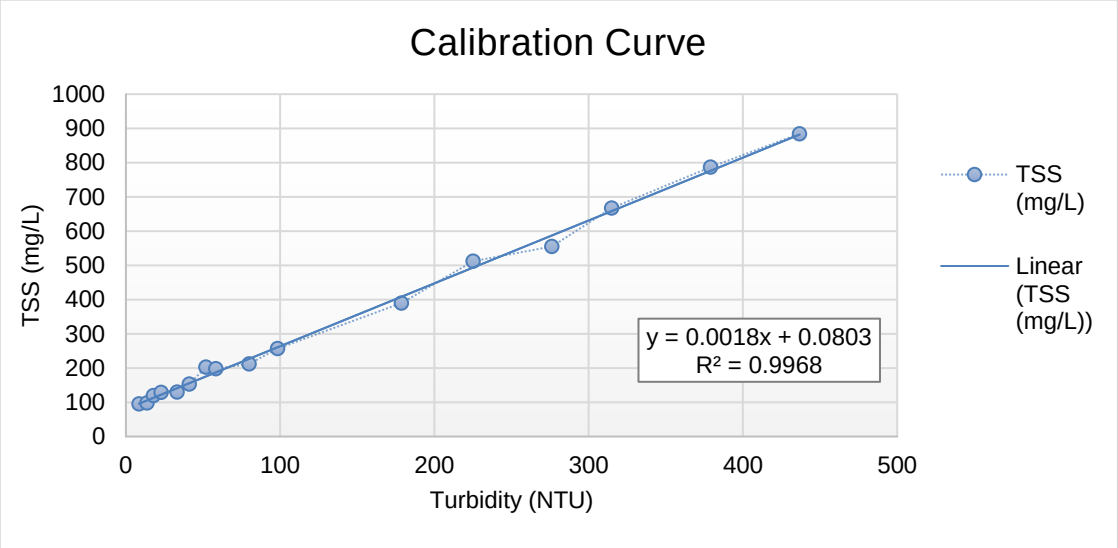

Figure 2 Calibration curve performed in-lab using CTD turbidity sensor.

Prior to running the calibration, the sediment was sieved in order to obtain only the mud (silt and clay) fraction from the sample, which are generally what is suspended and thus measured during the deployment. The sediment was first filtered through a 250-microns sieve to remove larger shells, etc. and then through a 63-micron sieve to remove the sand fraction. The sediment and water that passed through the filter was centrifuged and evaporated in order to obtain the mud fraction for the calibration. The number of tins and weight of sediment per sample added during the calibration were referenced from Minella et al. (2008) where they used around 10 to 15 samples containing between 0.25 to 2.5 g of sediment per tin. Similarly, 0.3 to 5.0 g of sediment were measured into 18 different tins. Around 10 L of the collected water was poured into an 18.93 L (5 gallon) polyvinyl bucket which was used to hold the water for the calibration. The turbidity sensors were attached to a pole and placed into the bucket. A paint stirring attachment was connected to an electric drill to allow for continuous homogenization of the bucket. The CTD was set to run on 6-Hz sampling. The paint stirrer was inserted to homogenize the water and after this became homogenized, a mud sample was mixed with 1 L of the water from the bucket and mixed back in. After a few minutes, the water-sediment mixture became equilibrated and around 400-600 mL of the water in the bucket was subsampled for filtering. The steps explained above were repeated 18 times in order to obtain a homogenized subsample after each tin was added. The subsamples were then filtered using the method described in Section 3.3 below.

3.3. Sample Collection

The Texas Corinthians Yacht Club (TCYC) pier located near Kemah, TX, was selected for our sampling location for suspended sediment from the middle bay (Fig. 1). The pier extends 470 m into the bay, with the water depth of 2 m at the end of the pier, permitting open water sampling. For a lower bay sample, the TAMUG Boat Basin was selected for ease of collection and being close enough to the mouth of the bay. There was not another pier accessible for water sampling. Sampling was conducted from September 2019 to February 2020. 60-80 L of bay waters in the two sites mentioned above within Galveston Bay (Fig. 1), depending upon the turbidity of bay waters, were sampled within 1-2 days after each storm event, conducted by attaching a bilge pump to a 4 m long, 3.81 cm diameter aluminum pole, with the bilge pump being mounted 10 cm above the bottom of the pole to prevent penetration into the sediment while still collecting suspended sediment from the bottom-water. Aliquots of the samples were filtered in the lab through a 0.45 μm polycarbonate filter for the measurement of total suspended particle (TSS) concentrations. The remaining samples were placed on the bench for a few days until the water was visibly clear of particles to allow the suspended particles sinking to the bottom of the containers, followed by the centrifugation to separate water from suspended sediments. Collected particulate matter from the centrifugation were dried in an oven at 50 ºC. The dried particles were ground and transferred into the gamma counting tubes for the measurement of ^{7}Be and ^{210}Pb.

Precipitation was collected on the roof of the Ocean and Coastal Studies Building (OCSB) at Texas A&M Galveston Campus. This location was chosen under the assumption that rainfall is relatively uniform throughout Galveston Bay. Based on

regular cold front patterns, they generally extend over the entire area of the bay. The rainwater was collected using a 20-L jug with a large funnel attached to the opening along with a 2-L bucket of water next to it for more collection. This was deployed before each rain event (Table 2). At the end of each storm event, the collected rainwater in all container will be combined for the extraction and analysis of ^{7}Be and ^{210}Pb (Section 2.3). Activity measurements of ^{210}Pb and ^{7}Be from rain water is necessary to perform the Matisoff method, to determine the "initial" age of the two radionuclides for each frontal passage event.

Table 1 OCSB measured precipitation (mm). Rain gauge measurement and amount of precipitation recovered from TAMUG OCSB roof.

Date	Rain Gauge (mm)	Precipitation Recovered (L)
1/29/2020	2	0.3
2/13/2020	32	2.5
2/21/2020	2	0.25

3.4. Measurements of ^{7}Be and ^{210}Pb

For the rainwater samples, ^{7}Be and ^{210}Pb were extracted from the collected precipitation based on the published method from Olsen et al., (1985) and Wang et al., (2013). After the adjustment of pH to <2, a certain amount of Fe^{3+} carrier solution ($FeCl_3$, 5 mg Fe per L of sample) was added under stirring. After homogenization and equilibration overnight, pH was adjusted to 9 with ammonia solution to precipitate the iron and $Fe(OH)_3$ containing ^{7}Be and ^{210}Pb overnight. The $Fe(OH)_3$ precipitate was

collected through centrifugation and dissolved by 3M HCl solution. Extracted samples from precipitation and the ground sediments from bay waters were placed into gamma counting tubes for analysis by a Canberra ultrahigh-purity germanium well gamma detector at the decay energies of 46.5 kev for ^{210}Pb and 477.6 kev for ^{7}Be. The sediment samples were counted again after three weeks to allow secular equilibrium ingrowth of gaseous ^{222}Rn from the decay of ^{226}Ra, the parent nuclide of ^{210}Pb. The supported ^{210}Pb was determined from the activity of the ^{214}Bi from the ^{222}Rn, at the decay energy of 609.3 kev. The atmospherically derived ^{210}Pb in suspended sediments ($^{210}Pb_{xs}$) was determined based on the difference between total activity of ^{210}Pb and the supported ^{210}Pb.

All samples were counted for 24 to 48 hours to obtain counting errors <10%, which is obtained from the gamma counter at the end of counting time. Counting efficiencies were determined, using the standards prepared with the same geometries as the samples. Activities concentrations of ^{7}Be and $^{210}Pb_{xs}$ were decay-corrected to the date of collection before the calculation of residence times.

3.5. Hotblock Acid Digestion Method

Due to low activity ratios of $^{210}Pb_{xs}$ in two precipitation samples (1/29/2020 & 2/21/2020), the hotblock acid digestion method was used (Kuehl et al., 2017). The two water samples were weighed and placed into a hotblock container. The weight of the precipitation samples prior to digestion is necessary to calculate dpm/kg. While the hotblock was being preheated, 25 mL of ^{209}Po tracer was added, followed by 15 mL HNO_3 and 15 mL HCl. The sample heated in the hotblock at 165^{o}C for 30 minutes. To prepare the silver planchet for the Alpha counter, 50 mL of diluted HCl and 5 mL

ascorbic acid were added and the set to stir for approximately 24 hours. After the 24 hours, the silver planchet is removed and cleaned with acetone and deionized water and set to count in the Alpha counter for 24-48 hours to reduce counting error below 10%. ^{210}Pb activity were calculated from the recovery of ^{209}Po and ^{210}Po.

3.6. Estimate of residence time of suspended sediments

Due to the significant difference in half-life between two radionuclides (53.3 days for ^{7}Be vs. 22.3 years for ^{210}Pb) and their strong binding to particles after their delivery from the atmosphere to the surface, the ratio of ^{7}Be over the atmospherically derived ^{210}Pb ($^{210}Pb_{xs}$) can be an indicator of the extent of mixing of freshly derived (^{7}Be enriched) suspended sediment with old (^{7}Be deficient) sediment resuspended from the bed of the Galveston Bay. Therefore, the $^{7}Be/^{210}Pb_{xs}$ ratio in the atmospheric deposition during the storm events is defined as the atmospheric tag received by the 'newly tagged sediment' in the Galveston Bay (Matisoff et al., 2005). Based on the variability of $^{7}Be/^{210}Pb_{xs}$ ratio in suspended sediments relative to the atmospheric $^{7}Be/^{210}Pb_{xs}$ ratio, the residence time or the age of suspended sediments can be estimated, across the middle Galveston Bay to the lower bay, based on the following equation:

$$\boldsymbol{T} = \frac{\boldsymbol{-1}}{(\lambda_{^{7}Be} - \lambda_{^{210}Pb})} \boldsymbol{ln}\left(\frac{\boldsymbol{A}}{\boldsymbol{B}}\right) + \frac{\boldsymbol{1}}{(\lambda_{^{7}Be} - \lambda_{^{210}Pb})} \boldsymbol{ln}\left(\frac{\boldsymbol{A_o}}{\boldsymbol{B_o}}\right) \quad (1)$$

Where T is the age of suspended sediment; A and B is the activity concentration of ^{7}Be and ^{210}Pb in the suspended sediments, respectively; A_o and B_o is the activity concentration of ^{7}Be and ^{210}Pb in the precipitation, respectively.

Furthermore, the percentage "new" particles in suspended sediments, which is defined as the sediment particles that have a $^{7}Be/^{210}Pb_{xs}$ ratio equal to precipitation, can be directly proportional to the $^{7}Be/^{210}Pb_{xs}$ ratio:

$$\%'\boldsymbol{new'sediment} = \mathbf{100}\,\boldsymbol{x}\,\frac{(\boldsymbol{A/B})}{(\boldsymbol{A_o/B_o})} \qquad (2)$$

3.7. Grain Size Analyses

Table 2 Grain Size Analyses of the TAMUG-TRIN station and TCYC sampling site via Malvern Mastersizer 2000®.

Sample	Sand (63-2000 µm)	Silt (4- 63 µm)	Clay (0.01-4 µm)
TRIN	76%	17%	7%
TCYC	87%	8%	5%
% Difference	13%	55%	26%

Grab samples were collected from the TAMUG-TRIN station during the first deployment and from the TCYC sampling site on 9/25/2020. These samples were homogenized and a small portion was sub-sampled for analyses. The sample preparation for grain size analyses involves mixing the sample with a dispersant composed of Sodium Metaphosphate and water. The combined slurry was poured in the Malvern Mastersizer 2000®. Five trials of each sample were placed in the Malvern for analyses to have an averaged value for thorough comparison. This device uses laser diffraction to

quantify the distribution of sand, silt, and clay components of each sample. From this, the percentage of each component was used to obtain a percent difference comparing both sites' sediment composition.

4. RESULTS AND DATA

4.1. Precipitation and Meteorological Data

Figure 3a displays total precipitation from Scholes Field in Galveston, TX comparing to the isotopic data collected in the lower bay and Figure 3b compares the total precipitation from the Dickinson Station to the isotopic data from the middle bay. The two meteorological stations were chosen based on their proximity to the respective sampling stations. Total precipitation data (Fig. 3) was collected from the National Weather Service (NWS) Forecast Office for the Houston/Galveston, TX area. Tidal data was collected from NOAA's Eagle Point, TX Station where water height was measured to Mean Sea Level (MSL) (Fig. 4). Salinity data on the right y-axis was obtained from the Texas Water Development Board's TRIN Station located in Trinity Bay from January 1st, 2020 to February 5th, 2020. The remaining salinity data was obtained from the TAMUG-TRIN deployment.

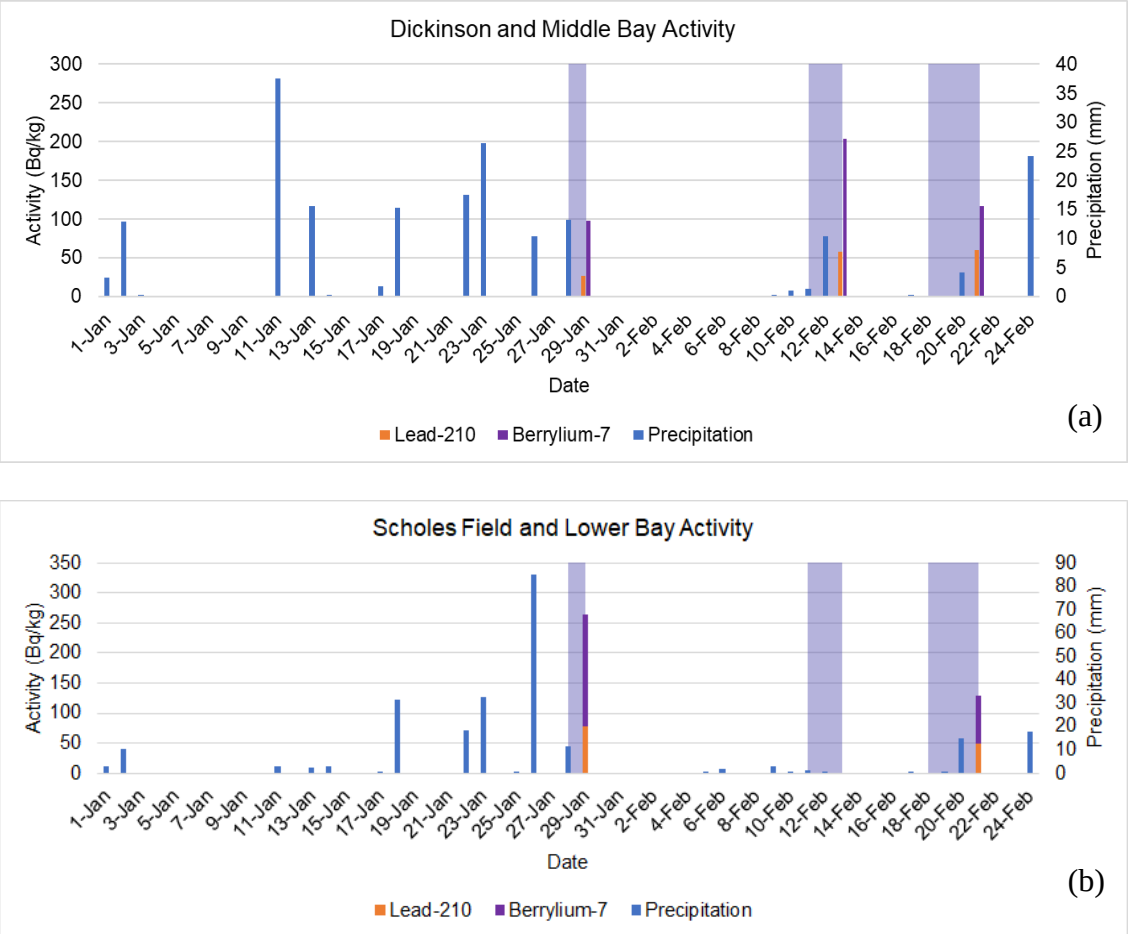

Figure 3 Rainfall vs. isotope activity. Rainfall data (checkered pattern) from Dickinson (a) and Scholes Field (b) Station (NWS) and isotopic activity of ^{210}Pb and ^{7}Be collected at the middle and lower bay site. Shading represents frontal passages.

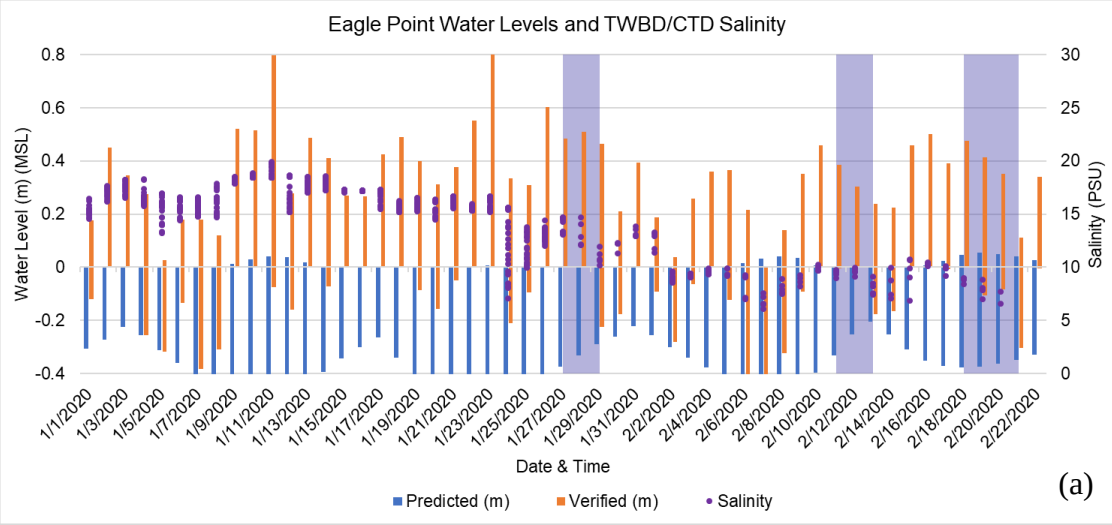

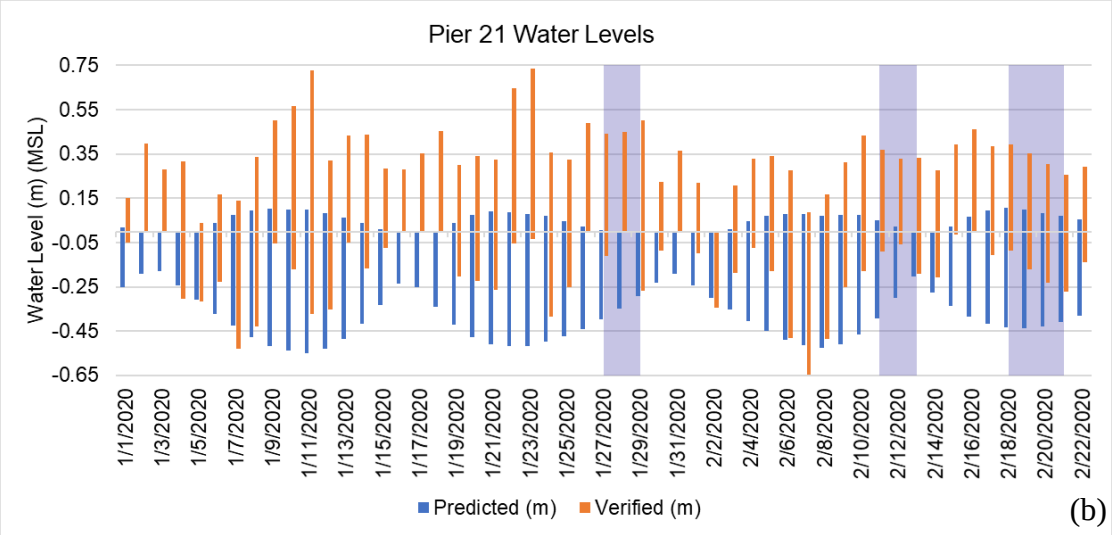

Figure 4 Predicted/verified water levels from NOAA Pier 21 and Eagle Point Stations. Predicted and verified water levels (m) (MSL) measured from NOAA Pier 21 Station for the months of January and February 2020. (a) Predicted and verified water levels (m) (MSL) measured from NOAA Eagle Point Station for the months of January and February 2020, (b) salinity (PSU) is obtained from Texas Water Development Board (TWBD-TRIN) station (1/1/2020-2/5/2020) and from the TAMUG-TRIN CTD station (2/6/2020-2/20/2020). Shading represents frontal passages.

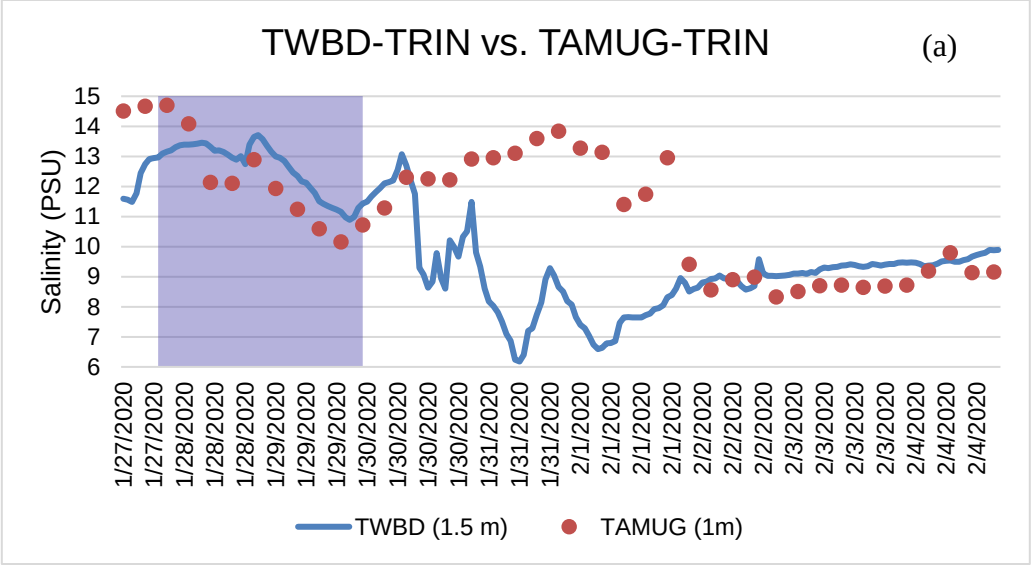

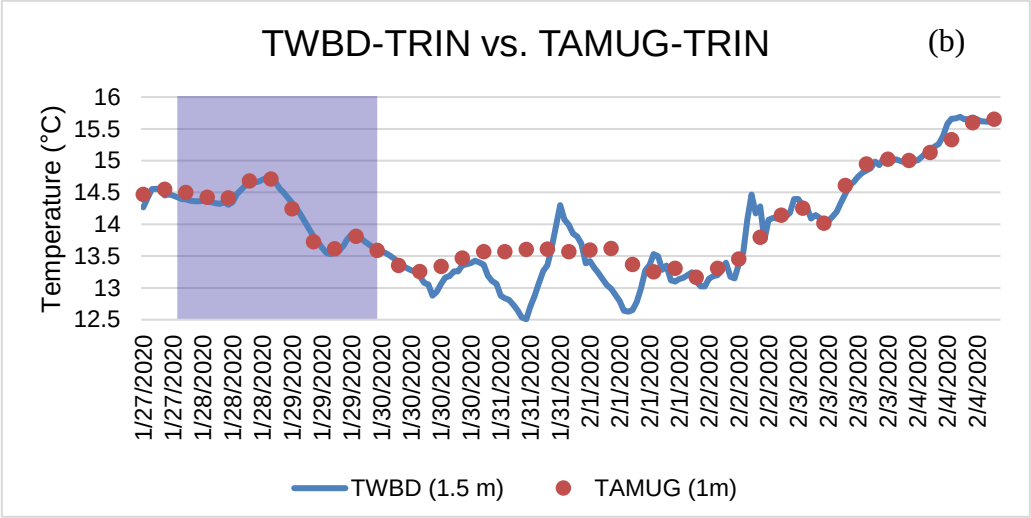

Figure 5 Comparison of TWBD-TRIN and TAMUG-TRIN salinity and temperature. Data measured from the CTD deployed in Trinity Bay compared to TWBD YSI located on same platform. (a) Observed (CTD) and TWBD YSI salinity vs. time. (b) Observed (CTD) and TWBD YSI temperature vs. time. Shaded area represents recorded frontal passage.

Data recorded from the CTD deployment in Trinity Bay were plotted and compared with a station from the Texas Water Development Board (TWDB) that was

mounted on the same platform as the CTD. (Fig. 1). The TWDB instrument was hung on the south-east corner of the platform and deployed at ~0.5 m water depth, where the average depth is approximately 1.5 m. The instrument deployed is a YSI 600OMS. Salinity and Temperature are measured on both instruments and plotted against each other above (Fig. 5). From January 30th to February 2nd, 2020, of the TWBD sensor, there was an instrument swap where the data logger was likely placed at a depth deeper than previously, which explains the lower salinity and large different from the CTD during this period. When it was swapped following February 2nd, it can be assumed that the instrument was placed at the original height from the beginning of data collection based on data above and comparing to the CTD salinity sensor. Data from TWBD only dates back to 2/5/2020, where the CTD was deployed until 2/21/2020, with biofouling being estimated around 2/8/2020, this makes for a reasonable comparison of instrument data collection. Meteorological data (e.g., wind speed/gusts, wind direction) was obtained from NOAA TCOONS station located within Galveston Bay (Eagle Point, TX) and plotted against TSS collected at the TAMUG-TRIN Station (Fig. 7). This station was chosen because it was the nearest station (26.02 km) to the TAMUG-TRIN Station that contained a meteorological data (Fig. 1). Figure 6 shows wind speed, gusts (m/s) and wind direction (degrees) data taken from NOAA Eagle Point, TX Station from the same dates that the CTD was deployed. The figure below (7) overlays TSS on top of the NOAA wind data.

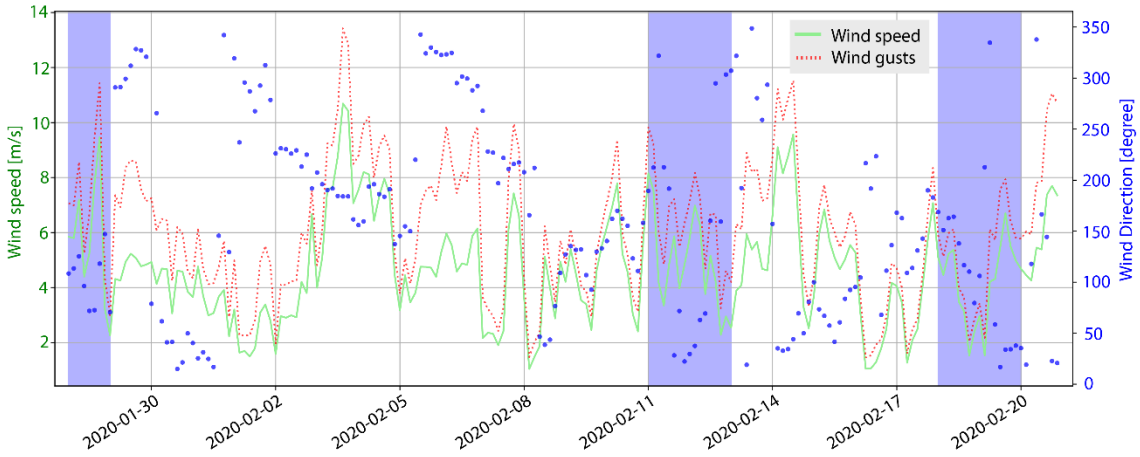

Figure 6 Measured wind speed, gusts, and direction from NOAA Eagle Point, TX. Wind speed, gusts (m/s) and wind direction (deg) vs. Time obtained from NOAA Eagle Point, TX station (https://tidesandcurrents.noaa.gov/met.html?id=8771450; https://tidesandcurrents.noaa.gov/met.html?id=8771013). Shaded area represents cold fronts.

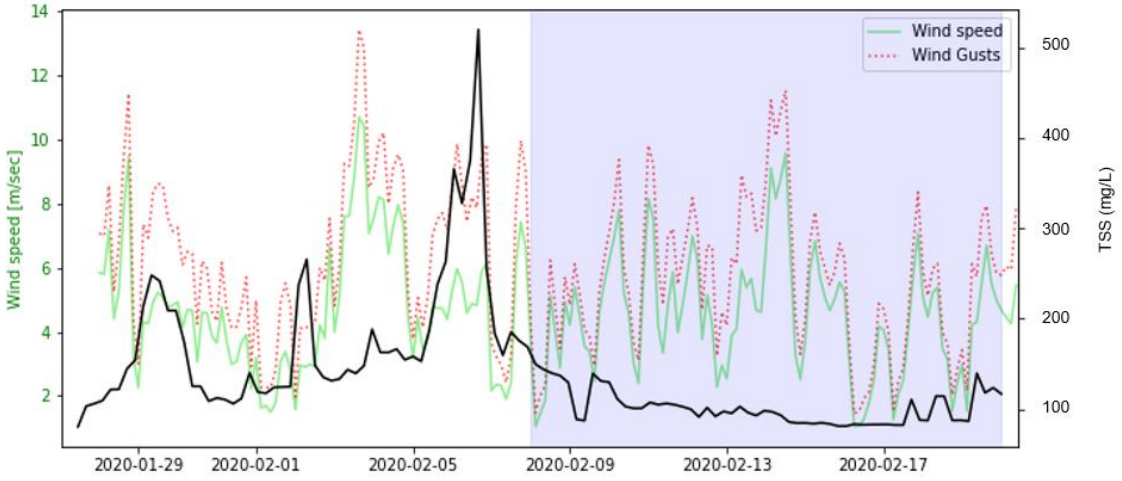

Figure 7 Wind speed, gusts (m/s) and TSS (g/L) vs. Time. Shaded area represents biofouling estimation.

4.2. TSS Results

TSS concentrations vary among the samples and are dependent of wind speed, wind direction, and tidal cycles (Table 3). Six of the samples were collected during flood tide and the other three were collected during ebb tide. During flood-tide, the water velocity is greater in the landward direction, whereas during ebb-tide it is greater in the seaward direction. Flood tide provides shorter, greater velocity, which produces a net landward transport of water resulting in more sediment resuspension, which can have more of an effect on the entirety of the bay (i.e the lower bay site) (Webster and Lemckert, 2002). Ebb tide has been stated to accumulate suspended sediment within an estuary, which in this case may also lead to higher TSS measurements during cold fronts at the mid bay site (Hossain et al., 2001). In addition to this, an ebb tide reduces the water levels within the bay causing wave energy to be greatly felt in the water column from wind waves produced from cold fronts, whereas flood tide increases water levels in the bay.

Table 3 Water sample collection data from the lower bay (TAMUG Boat Basin) and the middle bay (Texas Corinthians Yacht Club).

Boat Basin					
Date	**Time Collected**	**Tidal Phase**	**Wind Speed & Gusts (ms^{-1})**	**Wind Direction**	**Average TSS (mg/L)**
9/27/2019	11:30 AM	ebb	10 ms^{-1}	N/A	340
1/29/2020	3:00 PM	flood	6-7 ms^{-1}& 10 ms^{-1}gusts	WNW	90
2/21/2020	4:45 PM	flood	6 ms^{-1}& 7.5 ms^{-1}gusts	NNE	110
TCYC					
Date	**Time Collected**	**Tidal Phase**	**Wind Speed & Gusts (ms^{-1})**	**Wind Direction**	**Average TSS (mg/L)**
10/14/2019	11:00 AM - 1:30 PM	ebb	12.5 ms^{-1}	ESE	381
10/25/2019	1:00 PM - 2:00 PM	flood	7.5 ms^{-1}& 13 ms^{-1}gusts	NNW	64
11/12/2019	4:30 PM	flood	8 ms^{-1}& 11.5 ms^{-1}gusts	N	111
1/29/2020	1:30 PM	flood	6 ms^{-1}	WNW	109
2/13/2020	2:00 PM - 2:45 PM	ebb	6 ms^{-1}& 8 ms^{-1}gusts	N	114
2/21/2020	3:00 PM	flood	6 ms^{-1}& 10 ms^{-1}gusts	NNE	84

Comparing ebb tide versus flood tide solely with the middle bay, ebb tide correlated with the highest TSS concentrations, regardless of wind direction. When there was a flood tide, TSS is lower in the middle bay on 1/29/2020.In this case, the flood tide which was pushing water in a net landward direction in conjunction with a NNE wind. As previously stated, flood tide assists in resuspending more sediment, but in regards to the middle bay, the water levels become increased as opposed to an ebb tide. Although no TSS measurements were made at the lower bay station during an ebb tide frontal passage, due to both wave resuspension and tidal currents, it is assumed that sediment would be suspended during ebb tide with the lower bay as well.

In Galveston Bay, it was previously stated that sediment resuspension is heavily influenced by meteorologically driven shear stress rather than tidal driven shear stress (Dellapenna et al., 2006). This implies that winds created by frontal passages have a greater effect on TSS concentrations. Comparing wind speed/gusts and locations (middle bay vs. lower bay), TSS concentration at the middle bay station were higher on 1/29/2020 and lower on 2/21/2020. When frontal winds are at or below 6.0 ms^{-1}, it is less likely that TSS concentrations will be greater than 200 mgL^{-1}. The data suggests that northerly winds result in higher TSS concentrations at both sampling locations (Table 3). In the middle bay, a northerly wind combined with an ebb tide produced the highest TSS measurements, likely due to the combined currents and wind both aligned in the same direction during ebb tides, in addition to the reduction of water level, enhancing bottom shear. For the tropical storm sample (9/27/2019), the strong southerly wind coming into contact with suspended sediment coming from the north via ebb tide, can produce

similar results to a cold front with strong northerly winds (10/14/2019). During storms (1/29/2020 and 2/21/2020) where TSS was measured at both locations are close in value varying between 80-120 mgL^{-1}. For all samples collected in both the middle and lower bay site, it is observed when wind speed and gusts surpass a threshold greater than 6.0 ms^{-1}, TSS concentrations reach their maximum. Ebb tide was observed to have a greater influence on TSS than flood tide. Considering both the middle and lower bay, wind waves produced by strong frontal winds or those produced during coastal storms (>10 ms^{-1}) with an ebb tide, suspended sediment becomes the most concentrated within the water column.

TSS concentrations throughout the CTD deployment were between 80-500 mgL^{-1} (Fig. 6). The first TSS peak is followed by the cold front in late January, when wind speeds first shifted to a northern direction on 1/28/20 and increased from 6 to 8 ms^{-1}. The peak measurement of TSS was 247 mgL^{-1}, which correlated to a northern wind of 7 ms^{-1}. Prior to the first measured TSS peak, sediment remains in suspension, where the wind speeds decrease but remained from a northern direction. Wind speed reaches its highest value of 6 ms^{-1} with a south wind on 2/2/20, where TSS reached its peak as well. The consistent north wind possibly kept sediment in resuspension above 100 mgL^{-1}, and once wind speed rose above 5 ms^{-1}, despite the south wind, could have brought sediment into greater resuspension. Therefore, if sediment is already in suspension following a cold front, an increase in wind speed can keep sediments in suspension regardless of wind speed. Although, a northern wind created from cold fronts was seen to have a greater influence on resuspension. Lastly, the final suspended sediment peak in early February

corresponds with a northern wind with speeds varying between 4 to 10 ms^{-1} (Fig. 6 & 7). TSS reached its highest value during deployment of 519 mgL^{-1} accompanied by a northern wind gust of 10 ms^{-1}. This peak correlates to a winter storm, but there was no rain, therefore precipitation data could not be collected for isotope analyses. Following the final peak, wind speeds decreased and the wind direction shifted SW, where TSS concentrations subsequently decreased. From around 2/08 onward, TSS concentrations are greatly suppressed compared to the TSS concentrations during previous high wind events earlier in the time series (Fig. 7). When the pod was pulled, it was completely bio-fouled. The TSS concentrations spike for the cold front passages of 1/29-30 and 2/5-7, however, concentrations are significantly lower for the cold front passages of 2/13-15, and 2/20 and overall, the TSS concentrations are suppressed for the time series starting on 2/08. A barnacle settling event is likely the cause of the abrupt biofouling that suppressed the suspended sediment data recorded in the CTD, beginning on 2/8/20.

TSS concentrations from the TRIN Station were chosen based on sampling time being closest to that sampled at TCYC to conduct a comparison (Table 2). As mentioned above, significant biofouling appears to have started on 2/08, suggesting that the only reliable comparison for TSS concentration is from the middle bay (109 mgL^{-1}) and the TRIN (130 mgL^{-1}) pod location for 1/29/2020, where the difference is 16%. There was a flood tide during the measured event, suggesting that suspended sediments from Trinity bay did not mix with those sampled at TCYC. These concentrations indicate that the middle bay provides a fair estimate of suspended sediment concentrations for middle Galveston Bay, including Trinity Bay. Based on the grain size analyses via the Malvern

Mastersizer 2000, the three classifications of sediment types are generally similar, where the largest percent difference is silt (Table 2). With fine clays being the most common constituents for sediment resuspension, this leads to the assumption that the sediment type of the TAMUG-TRIN CTD site area is comparable to the sediment type at TCYC. Turbidity measurements are less subject to measurement error where biofouling is generally presented as the major error associated with the OBS sensor in a marine environment as seen in the data (Sidik et al., 2017, Matos et al., 2019). Most optical sensor display good performance with error ranging between 3-5% (Vousdoukas et al., 2011). The initial accuracy from the Seapoint OBS sensor is ± 1%, which has a minor effect on the data obtained. Therefore, the data collected provides a clear understanding of the relationship between wind speed, wind direction, and its subsequent effects on TSS increases and decreases.

4.3. Mooring Deployment

Figure 8 displays the CTD data collected during the TRIN Pod deployment. Salinity is lower during every cold front passage, which is likely the result of freshwater added to the bay from the associated rainfall events. During strong frontal events, subsequent mixing of the upper fresh water and lower salty water can occur (Fig. 8a). Following the first cold front event, salinity lowers to a minimum of 10 PSU two days after the initial rain event (1/26-28/2020), a likely result of the delay between rainfall and the time it takes for the drainage basin discharge to reach Trinity Bay. Salinity decreases again in conjunction with the TSS spike on 2/2/20, which was due to an increase in a southern wind, likely from subsequent wind-wave water column mixing.

The lowest salinity follows the rain event on February 13th (Table 2, Fig. 2), with which, as with the first event, there was a few days lag between the event and the associated recording of lower salinity at the pod site due to the rain event. Again, this was due to water column mixing, which was the greatest due to this storm being accompanied by the strongest northern winds, where wind waves had the greatest influence throughout the entire water column. Measured salinity becomes fairly uniform for the remainder of the deployment below 10 PSU, where just at the first two cold fronts, salinity begins to lower from the introduction of freshwater and winds from the cold front in late February. When comparing the two salinity sensors (Fig. 5a), the data follows a similar trend aside from a significant drop in the TWBD sensors' reading. It has been noted that when the sensor was replaced, the sensor was placed at a higher location than previously placed, allowing it to only collect data for the fresher top water. Overall, this comparison displays accuracy of measurements up to 2/05/20 for the CTD. The measured pressure from the CTD fluctuates throughout deployment. Pressure is lower than average during cold fronts. When wind speed increases, pressure decreases (Fig. 8b). The CTD conductivity measurements increase during the cold front events, aside from the measurements recorded from 1/28-1/30, which show an opposite trend.

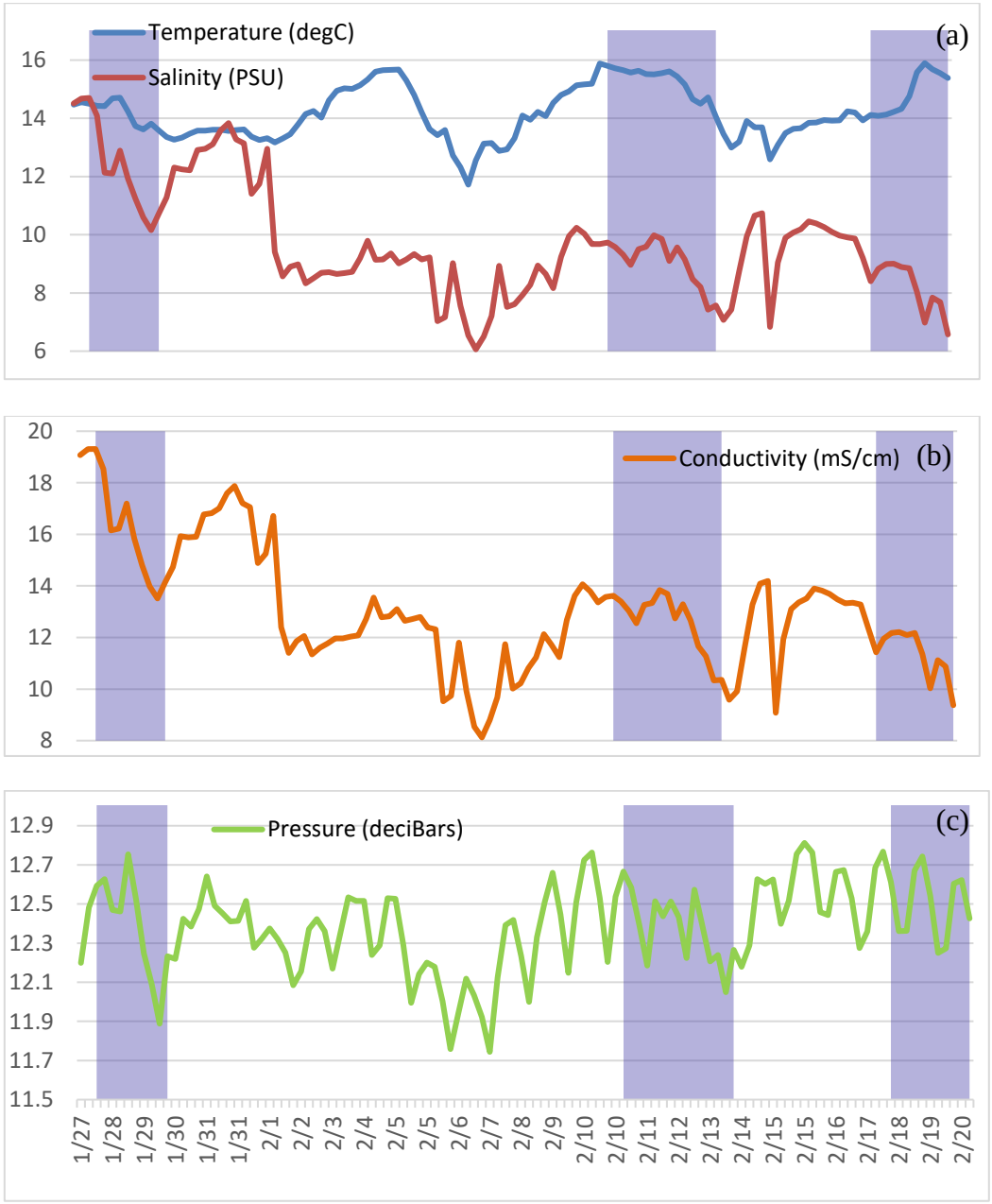

Figure 8 TAMUG-TRIN CTD measured parameters. Data measured from the CTD deployed in Trinity bay. Top to Bottom: (a) temperature and salinity (b) conductivity and (b) pressure vs. Time. Shaded area represents frontal passages.

Based on the comparison of the observed temperature from the CTD and the TWBD-TRIN Station, both instruments display a uniform trend (Fig.5). The decrease in water temperature follows the passage of the cold fronts (1/29-30,2/7-8, 2/13-15, and 2/20). Salinity decreases two days after the initial rain event and temperature follows the same trend. Following the first cold front event, the temperature remains between 13-14ºC for 5 days and increases by 4º C within another 2 days. This increase in water temperature follows the increase in a south wind, which also influenced TSS and salinity, which implies that there was water column mixing. This anomaly where the water temperature increases rather than decreasing can be attributed to the lack of precipitation along with the possibility that the south wind brought a water mass from an area of the bay that had an increased temperature. This water mass could have been from waters in shallower areas, such as closer to shore. Where in comparison, a north wind is likely accompanied by water from northern estuarine tributaries. The cold front beginning on 2/5/20 greatly reduced the temperature, which along with TSS and salinity results, implies the greatest impact of water column mixing. Similarly, to the cold front in late January, in mid-February the cold front reduced the water temperature by 1 ºC. From these two data points, it is assumed that the cold front in late February would decrease temperature as well. Despite biofouling disrupting the OBS sensor measurements beginning on 2/08/20, the other measured variables do not display the same trend.

4.4. Activities of ^{7}Be and $^{210}Pb_{xs}$ and Residence Times

Activities of $^{210}Pb_{xs}$ and ^{7}Be, shown in Table 4, were obtained from the gamma detector for sediment samples in both the middle and the lower bay along with precipitation samples from the TAMUG OCSB roof. ^{7}Be activities in all samples are higher than ^{210}Pb. This is likely attributed to the larger injection of ^{7}Be into the stratosphere, which enhances the stratospheric-tropospheric exchange, whereas ^{210}Pb is dependent upon the decay of ^{222}Rn into the atmosphere. (Olsen et al., 1985, Baskaran et al., 1993). Activities of ^{7}Be and $^{210}Pb_{xs}$ in bay waters during January 2020 were greater in the middle bay than the lower bay, whereas, during February 21, 2020, the opposite occurred. The highest activities for both the lower bay waters and precipitation can be seen on February 13, 2020, which also coincides with an ebb tide. The ebb tide water mass is derived from upper Galveston bay within estuarine tributaries, where this water is in more direct contact with drainage basin derived water. Therefore, newly deposited radioisotopes are rich within this water mass. In contrast, the flood tide water mass is marine derived, only receiving drainage basin water after mixing with the ebb tidal water mass. ^{210}Pb activity for all events is lowest in precipitation. This could be due to the entirety of ^{210}Pb flux in rainfall being solely from wet fallout, whereas in suspended sediment samples ^{210}Pb becomes remobilized from bottom sediment (Baskaran et al., 1993). Overall, activities of both radionuclides fluctuate throughout sampling events at all locations.

Table 4 $^{210}Pb_{xs}$ and ^{7}Be activities (Bq/kg) of sediment and precipitation samples.

		Middle Bay		Lower Bay		Precipitation (OCSB Roof)	
Dates	**Tide**	**$^{210}Pb_{xs}$ (Bq/kg)**	**^{7}Be (Bq/kg)**	**$^{210}Pb_{xs}$ (Bq/kg)**	**^{7}Be (Bq/kg)**	**^{210}Pb (Bq/kg)**	**^{7}Be (Bq/kg)**
1/29/2020	in	26 ± 2.7	98 ± 3.4	78 ± 8.0	186 ± 8.7	22 ± 1.9	205 ± 5.4
2/13/2020	out	58 ± 5.0	204 ± 6.0	Not Collected	Not Collected	44 ± 5.2	482 ± 7.4
2/21/2020	in	60 ± 6.0	117 ± 6.6	50 ± 5.2	79 ± 5.2	17 ± 1.5	63 ± 2.5

The anomalously high ^{7}Be measurements from the lower bay of 186 Bq kg^{-1} for January 29 compared to 79 Bq kg^{-1} for February 21, as well as the differences in the $^{7}Be/^{210}Pb_{xs}$ ratios need to be placed into the context of this large precipitation event. In the middle bay, the January 29 ratio of $^{7}Be/^{210}Pb_{xs}$, is nearly twice that for February 21, at 3.8. The city of Galveston was raised in 1911 so that it all drains north, nearly all of the runoff from the eastern 9 km of the island (18 km^2) flows directly into the Galveston Channel. Pelican Island extends along the northern side of the Galveston Channel and is a natural island which has been expanded through land reclamation. It appears that the southern 3.5 km^2 also drains into the Galveston Channel, for a total of 21.5 km^2 drain directly into the Galveston Channel. Wet and dry deposition are the primary sources of ^{7}Be to the environment (Williams et al., 2018), so, it is well established that during high precipitation events, that coastal water becomes enriched with ^{7}Be (Williams et al., 2018). Analyses of the activities of the precipitation from the OCSB roof rain collector is a bit counter intuitive. When it rains, the isotopes are stripped out of the atmosphere, so a

smaller event will actually have a higher isotopic activity than a larger event, but the overall load of the isotope to the watershed increases because of the larger volume of water delivered which contains the isotope (Williams et al., 2018). Because the atmosphere is also the source of ^{210}Pb, atmospheric stripping from precipitation can also explain these variations as well. Because the flow path between the watershed and the channel is so short (i.e., less than 3 km), there is a nearly direct input of the isotopes to the water column, for the Galveston Channel, with little opportunity for mixing or losses. However, the flow paths for the middle bay are on the order of 10's of km and there will be significant mixing both with waters from the watershed as well as within the bay prior to being sampled. Consequently, the higher ^{7}Be activities can be explained by the dramatically greater rainfall in Galveston versus Dickinson and short flow path for the Jan. 29 event for the Galveston Channel, which had a more direct delivery of larger isotope load than that of Galveston Bay proximal to the middle bay.

In relation to tidal phases, it is only possible to compare flood versus ebb tide in the middle bay. For both isotopes, activities are higher during ebb tide. The ebb tidal water mass is derived from the upper bay and from within the estuarine tributaries and this water is in more direct contact with the drainage basin derived water. In contrast, the flood tidal water mass is marine derived and receives drainage basin water only after mixing with the ebb tidal water mass. Consequently, the ebb tidal water mass is generally more enriched with drainage basin derived isotopes input through precipitation events than the flood tidal water masses. However, when we consider the water levels within the bay during January and February 2020 (Fig 4), we find that during much of

January, for the Eagle Point Station, which is 9.4 km southeast of the TCYC Pier (middle bay), the water level was at least 0.3 m above the predicted tide, was as high as 1.0 m above the predicted tide for much of the month. In addition, for the four days prior to the sampling, the water level was generally at least 0.5 m above the predicted tide. Although, for the February, prior to the cold front of Feb. 21, 2020, the water levels were also comparably elevated, for the two days prior to the water sampling event, the water levels were suppressed, approximating the Predicted Levels. It should be noted that often during and just after cold fronts, the water level in the bay can be 0.5 to 1.0 m below predicted tides. When we consider the water level in the lower bay, we can use the Galveston Pier 21 NOAA Station (Fig. 4b), which is also located within the Galveston Channel, 2.5 km to the east. The Pier 21 Station shows that similar trends to Eagle Point, but with overall water levels ~10-15 cm lower (Fig. 4a).

The $^{7}Be/^{210}Pb$ ratios of precipitation in Galveston for three years (1990,1991,1992); comparing similar months (Jan.-Mar.) from each year, ratios averaged between 15.4, 13, and 8.6, respectively, which are comparable to our ratios in precipitation (Table 5) (Baskaran et al., 1993). It was also found that the lower ratios in precipitation were contributed to continuous rainfall coming from the cold fronts that are enriched in ^{210}Pb versus oceanic air masses (Baskaran et al., 1993). With the maximum ratio in precipitation sample from mid-February, where the greatest amount of rainfall was collected, but not recorded at Scholes Field (Fig. 6b, Table 5). January 2020 has a similar ratio to mid-February 2020, but there was less rain collected and higher rainfall measurement from Scholes Field. The lowest precipitation ratio was found in late

February, which like the first, had the least amount of rainfall collected for sampling. According to Scholes field, the largest quantity of precipitation was measured in late February. When looking at the activities in precipitation of all three events, the lowest activity of both isotopes is found in the last storm (Fig. 3).

Table 5 $^{7}Be/^{210}Pb_{xs}$ ratios ± standard error calculated from activities of precipitation, suspended sediment samples with calculated suspended sediment age and percentage new sediment.

Date/Tidal Phase	January 29, 2020 (in)			February 13, 2020 (out)			February 21, 2020 (in)		
	$^{7}Be/^{210}Pb_{xs}$	Age (d)	% New	$^{7}Be/^{210}Pb_{xs}$	Age (d)	% New	$^{7}Be/^{210}Pb_{xs}$	Age (d)	% New
Precipitation	9.4 ± 0.8	0 ± 0	100 ± 9.0	11 ± 1.2	0 ± 0	100 ± 12	3.7 ± 0.4	0 ± 0	100 ± 9.5
Middle Bay	3.8 ± 0.5	70 ± 10	40 ± 5.6	3.5 ± 0.5	86 ± 13	32 ± 5.0	2.0 ± 0.3	51 ± 8.0	52 ± 8.0
Lower Bay	2.4 ± 0.4	105 ± 15	25 ± 3.6	Not Collected			1.6 ± 0.2	67 ± 10	42 ± 7.0

When considering the variations in the $^{7}Be/^{210}Pb_{xs}$ ratios in sediment (Table 5), the January sample had a ratio for the middle bay that was 1.6 times higher than the lower bay. In contrast, for the late February samples, the middle bay has a ratio that is 0.8 times higher than the lower bay. The ratios of suspended sediment previously recorded in the Gironde estuary had comparable activity ratios of bottom sediment

averaging at 1.5, which was most closely similar to the lower Galveston Bay site (Table 5; Saari et al., 2010)., both the Gironde and the lower Galveston Bay sites were proximal to the respective bay mouths and the ocean (Fig. 9). Lower ratios in suspended sediment can be from the reintroduction of ^{7}Be-dead sediment, which is more commonly found below 2 cm into sediment column. During times of strong sediment resuspension, this can be reintroduced into the water column along with older ^{210}Pb. This can be possible when measuring suspended sediment. For the mid and lower bay, this is not as likely even during frontal events, unless measurements were taken from where scouring may occur (i.e., wooden pilings). Additionally, reintroduction of ^{7}Be-dead sediment and older ^{210}Pb would also result in lower activities, which is not the case in any samples. It is expected that the highest ratios would be found in rainfall followed by suspended sediment in "upstream" areas, like the middle bay, followed by suspended sediment in "downstream" areas (e.g., lower bay). All three-sampling events follow this trend throughout the Galveston Bay system (Table 5).

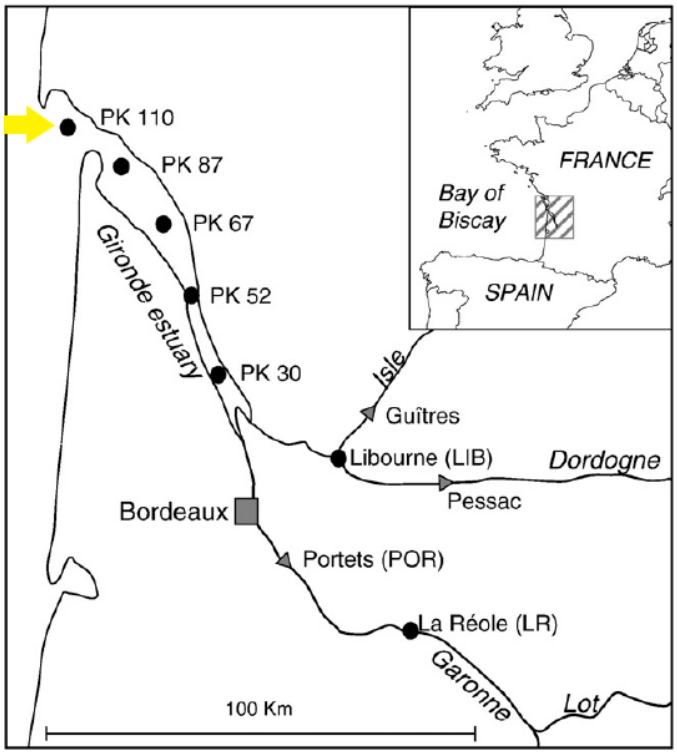

Figure 9 Gironde estuary sampling where particulate sample comparison is located by the blue arrow (Saari et al., 2010).

Regarding age and percent new of suspended sediments, our results show that age increased and percent new decreased along the axis from the upper/middle bay to the lower bay (Fig. 10). Throughout the three events, the age of the suspended sediment in mid-February 2020 is the highest, followed by late January 2020, then late February 2020. The percent new are different from this, with the lowest percent new occurring with the mid-February 2020, sample, followed by late January 2020, and the highest percent new for late February 2020 samples. There is not a comparable trend for the ages of the suspended sediment because age is a function of the introduction of fresh isotopes.

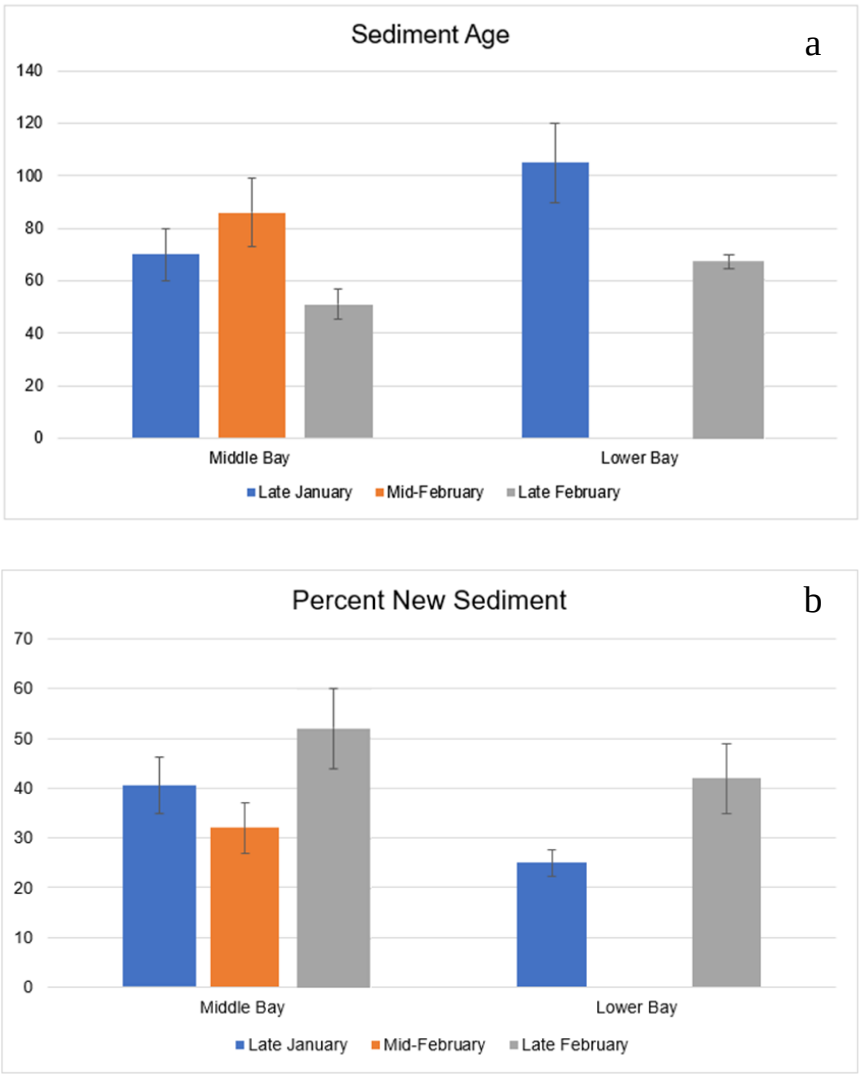

Figure 10 Age of suspended sediments (a) and percent "new" sediments (b) in middle and lower Galveston Bay during three cold front events in 2020.

Matisoff et al. (2005) measured the ages of suspended sediment and the percent new for three catchments (Table 6), all within the US National Estuarine Research Reserves, they are: 1) Weeks Bay which is small 7 km^2 embayed into the eastern shore of Mobile Bay; 2) South Slough, is small estuary off of Coos Bay in OR, USA; and 3)

Old Woman Creek, a lake/fluvial system (lacustrine equivalent to an estuary) that empties into Lake Erie along its southern shore, in Ohio, USA. Weeks Bay is most comparable to Galveston Bay in terms of environments, both are shallow estuaries along the northern Gulf of Mexico. In addition to bay characteristics, water residence time in Galveston Bay has been measured to be about 40 days (Du et al., 2019), and is estimated to be 13 days in Weeks Bay (Novoveska and MacIntyre, 2019, Solis & Powell, 1999) and 8.5 days in Old Woman Creek (Matisoff et al., 2005). Galveston Bay is two orders of magnitude larger than either Weeks Bay or Old Woman Creek, and so it would be expected that the residence times would be longer. In contrast, the age of suspended each bay is much longer, with the age of the suspended sediment in Weeks Bay estimated to be 79 days; in Old Woman Creek, 104 days; South Slough, 93 days (Matisoff et al., 2005); and Galveston Bay was found to range from 51-86 days. It should be noted that the age of the suspended sediment is not the duration of time that the sediment has remained suspended in the water column, but rather the duration of time that the sediment is either susceptible to resuspension, i.e., either sitting at the or very near the seabed surface versus either exported out of the bay or buried to a depth below which it is no longer available for resuspension. If the water column residence time is longer than the age of the suspended sediment, then the suspended sediment is either buried or exported out of the bay within a single residence time. If, in contrast, the suspended sediment age is longer than the residence time of the bay water, then that means that the sediment is trapped, but still available for resuspension for a longer multiple residence time cycles. If we divide the age of the suspended sediment by the water column

residence time, the ratio produced is an estimate of the retention/export efficiency of the suspended sediment within the estuary. A higher value indicates that the suspended sediment is retained and available for sediment resuspension for a longer time and a lower value indicates either more rapid burial to below a depth of resuspension or a more rapid export from the bay. This ratio was calculated for Galveston Bay, Weeks Bay and Old Woman Creek. Table 6 reveals that of these three systems, the suspended sediment of Galveston Bay was available for resuspension for 1.28-2.15 water column residence times, whereas the suspended sediment within Weeks Bay was available for 6.1 water column residence times. If we divide the number of residence times needed to trap or export sediment for Weeks Bay by the same parameter for Galveston Bay, we see that Galveston Bay is 2.8 to 4.7 times more efficient in either trapping or exporting its sediment than Weeks Bay.

Table 6 Summary of areas, water residence times, age and % new suspended sediment.

System	Area of Estuary	Water Residence Time	Age of suspended Sediment	%New Suspended Sediment	Water Column Residence Time/Age of Suspended Sediment
Galveston Bay	1,397 km^2	40 days[2]	51-86 days	25-52%	1.28-2.15
Weeks Bay[1]	24 km^2	13 days[3]	79 +/-8 days	36% +/-4	6.1
South Slough[1]	19 km^2	n/a	93 +/-9 days	30% +/-4	n/a
Old Woman Creek[1]	2.3 km^2	8.5 days[1]	26+/-3 days	26% +/-3	3.1

[1](Matisoff et al., 2005). [2](Du et al., 2019). [3](Herdendorf et al., 2004)

4.5. Sediment Transport in the bay

The Matisoff et al., (2005) relationship works because the younger isotopes are introduced via precipitation both via fluvial runoff to the bay where the suspend load of sediment is isotopically labeled with a young age. In contrast, precipitation in the bay resides within the fresher surface water while the bottom waters are isotopically older and have a higher salinity. As a result, resuspended sediment within the bay will, in general, have an older age than newly introduced suspended load from the fluvial systems. Because the head of the bay is where the largest fluvial systems discharge, the $^{7}Be/^{210}Pb_{xs}$ ratio is expected to decrease as isotopes travel through a system (middle bay to lower bay). This statement assumes that suspended sediment is being advected through the bay along the salinity gradient. This is true for late January and mid-February 2020, where data collected from the middle and lower bay have a decreasing $^{7}Be/^{210}Pb_{xs}$ ratio and sediment age for late January and late February 2020 increase closer to the mouth of the bay, confirming the hypothesis that sediment age should increase as suspended sediment moves through an estuarine system. In addition, the percent/fraction of new sediment decreased as age increased which is seen in Table 5 for both January and late February samples. A lower bay sample was not collected in mid-February 2020, but based on the other two storms, it would be assumed that the sample in the lower bay would follow the same trend. The older age in both samples from the lower bay results in both because the location is distal from large sources of freshly labeled suspended sediment from upper bay that is mixed with older resuspended bay sediment. This study validates the application

of $^{7}Be/^{210}Pb_{xs}$ to determine the age of sediment in Galveston Bay. Although, with the variability of water transport and trapping within Galveston Bay, the values found can only be used to observe the bigger picture of the overall sediment transport. Please note that the time of year and characteristics of meteorological events can alter the data presented here.

In order to understand what these trends mean in Galveston Bay; we need to investigate what was going on in the bay in regards to water levels and salinities during the weeks preceding the sampling. Based on the analyses of the water levels when compared to the predicted tides, we find there was a large influx of flood water trapped within the bay during much of January 2020 and when we consider the conductivity data from the Eagle Point Station, we find that conductivity was reported between 20-23 mS/cm from Jan. 1-12, 2020, when the station went offline (Fig. 5b). It comes back online on February 25, 2020 at 10.22 mS/cm. When we consider the salinity reported from the CTD from the pod deployment (Fig. 5), for the month of January, salinity ranged between 19 and 10 PSU, but with the total amount of rainfall for the month of January in Dickinson being 200 mm, it would imply that the salinity would be much lower than this. This indicates that there was a greater mass of higher salinity marine derived water that was trapped within Trinity bay.

Then on January 28th, salinity was observed to be between 13-14 PSU and progressively decreased to below 10 PSU following the cold front in late January, 2020. Following this rain event, and the remainder of sampling, the salinity does not rise above 11 PSU (Fig. 5a). This indicates that high salinity water mass was flushed following the

cold front in late January towards the mouth of the bay. By the time of the water sampling on Feb. 13th, the age of sediment was older than before, implying that the high salinity water mass had yet to exit the bay but had moved further towards the mouth of the bay. Unfortunately, there is not a salinity sensor in the lower bay. In a 3D modeling study of the hydrodynamic circulation found that in general, Trinity Bay has weak tidal currents (Du et al., 2020). Due to these weak currents, water masses can be trapped within Trinity Bay for prolonged periods of time. This appears to be the case for much of January 2020 and mid-February 2020, and may help explain these salinity trends. Based on this observation, there are longer residence times of unflushed water, leading to longer residence times of suspended sediment within these water masses. Older suspended sediment from January 2020 was still present in mid-February where the age was 16 ± 3 days greater than late January. In addition to an older age in mid-February, the percentage of new sediment was 8 ± .6% lower than January 2020 (Fig. 10). Where in late February, it appears that the majority of the sediment measured in mid-February was transported entirely out of the bay from this cold front leading to the age in late February to be 35 ± 7.4 days younger (Fig. 10). The younger age was from a greater abundance of new particles versus old/dead nuclides became more predominant in the middle and lower bay sediment that was measured in late February 2020. The data presented here displays that cold fronts have the ability to resuspend and transport sediments, but with the hydrodynamic trapping of water masses within the bay (e.g., Trinity River), the length of time sediment reside within the bay may vary.

In addition to the trapping of higher salinity water in Galveston Bay in January, there were also significant differences in precipitation between the months of January and February (Fig. 3). Two meteorological stations were analyzed for rainfall data, Scholes Field, which is located on 14 km west of the eastern end of Galveston Island and the Dickinson Station, located 10 km southwest of the TCYC Station. The total rain fall for Scholes Field and the Dickinson Station are shown in Table 7, note, the total for February for the Dickinson Station, the station record reported its precipitation event was on Feb. 24, after the sampling event of Feb. 21, so this rainfall was subtracted from the total for this station. These data reveal that the rainfall total for Scholes field is nearly an order of magnitude greater in January than February and for the Dickinson Station more than an order of magnitude greater in January. At Scholes Field, the rain gauge recorded an event on Jan. 26 which resulted in 93.98 mm of precipitation. Although precipitation in Dickinson was high that day, it did not even reach the high for the month, which was nearly a third less than the Scholes Field event. In fact, this event led to significant street flooding throughout the city of Galveston.

Table 7 Rainfall data from Scholes Field and Dickinson Station obtained from NWS.

Station	**Scholes Field (Galveston)**	**Dickinson (Mid-Bay)**
January 2020 Total	200.66 mm	153.92 mm
Jan. Highest Event	93.98 mm (Jan. 26)	37.59 mm (Jan. 11)
February 2020 Total	38.35 mm	17.3* (41.40 mm)
Feb. Highest Event	19.30 mm (Feb. 12)	24.1 (Feb. 24)

Note: The highest event for February for the Dickinson Station was after the sampling event was collected, so is subtracted from the Monthly total for February.

4.6. Implications to the bay environment

Estuaries and coasts are known to be the primary filter between the land-sea margin, where rivers and estuaries serve as sources of particulate contaminants to coastal environments (Huang, Du, and Zhang, 2011). With Galveston Bay being a microtidal environment, residence times can be longer due to less water transport from tides, especially during low flow/water discharge. The heavy metals and different organic pollutants that quickly sorb to settling particles become the "sink" of an estuary. With nearly the entirety of Galveston Bay being highly industrialized, it is likely that an abundance of pollutants/chemical constituents reside within the bottom sediment. For example, surface sediment was measured in Galveston Bay and it was found that various particle reactive metals (e.g., lead, barium, mercury, copper, manganese, zinc, etc.) and polycyclic aromatic hydrocarbons (PAHs) sorbed onto the sediment, meaning that they have a great chance of resuspending during resuspension events (Santschi et al., 2001). Therefore, our estimated residence time of suspended sediments (51-105 days, Table 2)

suggest these pollutants that adsorb to suspended sediment may spend months before they leaving the Galveston Bay. The long residence times of sediments in Galveston Bay will increase the exposure time of living organisms to various pollutants. Along with the trapping of water masses that potentially allow for the accumulation in organisms will affect the health of Galveston Bay. Additionally, although cold fronts or other storm events can enhance sediment transport (i.e., reduce the residence time of suspended sediment), their induced sediment resuspension will result in the continuous interaction of the sedimentary pollutants with the water column of Galveston Bay, which loosely adsorbed pollutants in sediments may be released back to the Galveston Bay waters. In contrast to the potential negative impact from long resident time and resuspension of bay sediments, some positive feedback may be beneficial to the bay environments, such as the nutrients release from the sediment resuspension (e.g., phosphate, Lin et al., 2013; Chao et al., 2017; Guo et al., 2020), which can promote the phytoplankton growth and accelerate the ecosystem function in Galveston Bay. Thus, $^{7}Be/^{210}Pb$-assisted investigation of sediment dynamics and age will help us better monitor the environmental quality in estuarine systems. Another factor this study brings to light is the ratio of the residence time of the water column to the residence time of the suspended sediment. The residence time of suspended sediment is an estimate of the duration of time that the sediment available for resuspension before either exiting the bay or being buried to a depth below which it can be resuspended. The more water column residence times that particle reactive contaminant labeled sediment resides within the estuary, the greater the opportunity that pelagic organisms moving with the

water column have to be exposed to these particle reactive contaminants. It is not just the long residence time of the suspended sediment that is a factor, but also the amount of water column the particle reactive suspended sediment is exposed that is the risk to the environment.

4.7. Limitations and Advantages/Drawbacks of Methodology

Due to the powerful nature of cold fronts (strong winds, waves, etc.), the ability of sampling on a boat in the middle of middle and lower Galveston bay was not possible. Therefore, the middle bay pier, was selected because it extends 0.47 km into Galveston Bay, permitting easy access to open bay waters. The samples were collected at 0.35 km from shore, in approximately 2 m of water, allowing for a reasonable middle of the bay sampling station. It should be noted that samples collected further into the bay would likely have been more representative of open bay conditions, but such a site was not available. Unfortunately, the higher mounted turbidity sensors' readings were invalid. Therefore, only one sensor was used for data analyses.

During sampling at both locations, the tide was flooding aside from Feb 21st 2020 in the lower bay. For the middle bay, the tide was ebbing during sampling on October 14th 2019 and February 13th 2020. This may affect comparisons of TSS measurements between locations and dates, however, the timing of the passage of the front was out of our control. Wind speed and gusts during sampling ranged from 4 m/s to 10 m/s with gusts ranging from 8 m/s to 14 m/s. Wind direction was generally out of the N, NNW, and NNE for cold fronts and came from the S-SE during the tropical storm measured on September 2019 (Fig. 7).

Rain data was solely collected at one location, being the roof of OCSB located on the TAMUG campus. Cold front events generally effect the entire bay; including rainfall allowing for a singular precipitation collection location when using the same data to compare to the middle bay. Although, the measurements of rainfall from Dickinson station and the Scholes field station greatly varied, leading to the assumption that rainfall is not uniform throughout the entire bay and the values obtained can only be used to observed sediment transport in terms of isotopes in a bigger picture. The amount of rainfall varies per cold front; therefore, activities of isotopes vary as well. Due to the small amount of rainfall collected for January 29th and February 13th, ^{210}Pb activity was too low to be detected in the germanium gamma detector. Because of this, ^{209}Po method was used to find the activity of ^{210}Pb. The ^{210}Pb concentration in rainfall was significantly lower than ^{7}Be. The difference in the concentrations altered the residence time calculations and activity ratios. It is preferable to wait 1-2 years to measure ^{209}Po in the Alpha counter in order to let Po grow and find the equilibrium for ^{210}Pb and ^{209}Po. Therefore, the planchets can be measured again to estimate a higher concentration of ^{210}Pb activity. For the January 29th precipitation activity of both ^{7}Be and ^{210}Pb, an average of two activities was taken, the second activity was from measured activity of both isotopes on January 22nd. This allowed for calculations of age and percent new that were not negative or over 100%, respectively.

Another limitation included the variability of cold front events. For this study, there were a total of 6 cold fronts to sample. During CTD deployment, 2 of the 6 were recorded. In relation to the number of cold fronts recorded, TSS collection began in Fall

2019. Unfortunately, accompanying precipitation samples were not being collected until January 2020, making the Matisoff method not applicable during the first 3 cold front events sampled. Although additional pod deployment had been planned, the shutdown due to COVID-19 crisis precluded additional deployments and sampling events.

5. **CONCLUSIONS**

The stronger the wind speed the higher TSS concentrations become, especially with a northern wind direction. This confirms the hypothesis that stronger winds are attributed to higher TSS due to more sediment being resuspended from the bottom by wind waves. Samples collected during ebb tide displayed higher TSS concentrations, likely the result of the addition of tidal current coupled with wind waves and wind-driven current and ebb tide reducing water levels in the bay imparting greater shear stress to the seabed. Northerly components of winds are dominant during cold fronts; and in estuaries result in a down-basin transfer of water and suspended materials (Booth et al., 2000). It was assumed that this would cause TSS to always be higher in the middle bay, but based on the data, ebb and flood tide influence TSS such that it is not case. The reduction of water levels allows such wind waves from cold fronts to impart greater shear stress on the seabed. Although, more sampling throughout the year needs to be conducted in order to have a greater support and spread of varying factors controlling TSS. From the data, it can be inferred that it is likely that an ebb tide along with a northly wind can generate the highest TSS measurements.

Throughout the CTD deployment, TSS concentrations ranged from 80-500 mg L^{-1}. The highest sediment resuspension in Trinity Bay correlates with a strong north wind. Concentrations fall below 200 mg L^{-1} when wind direction changes from northern to west and southeast winds unless such winds accompany a speed greater than 5 ms^{-1}. This may also be due in part to a cold front that previously resuspended sediment and the sediment remained in suspension, where suspension increased again when wind speed

increased, in this case due to a southerly wind. It is possible to suggest that sediment resuspension is more likely to occur during the frontal phase when winds are north, northwesterly, or northeasterly. Knowledge of sediment resuspension timing and intensity during cold front events is important when trying to understand transport of sediment and adsorbed materials (e.g., nutrients, contaminants, etc.). The strong impact and frequency of these meteorological events makes it important to understand such processes.

The residence times/age of suspended sediment increases as suspended sediment moves towards the mouth of the bay (Table 5). Based on the results, it is observed that the mid-bay suspended sediment is younger than the lower-bay, suggesting that the hypothesis was confirmed. Despite the data found, Galveston Bay is highly variable in terms of water transport and trapping meaning that sediment transport may be different from isotope transport at times. Based on each individual storm, activities are higher in the lower bay than in the middle bay, aside from the last measured cold front (2/21/2020) and in every measured sample, ^{7}Be activities are higher than $^{210}Pb_{xs}$, which is most largely attributed to abundance of rainfall. In order to fully understand the activities of ^{7}Be and $^{210}Pb_{xs}$ when used to find residence time/age of suspended sediment, additional samples need to be collected during the fall cold front season (October-December). There are many factors to observe when understanding the transport of sediment/particles throughout an estuarine system such as total precipitation and salinity. Based on the results mentioned above, it is observed that repetition of large rainfall events within a short time period (i.e., one month) lead to the flushing of high salinity

water leads to the largest release and greatest mixing of sediment from the upper/mid-bay.

This study demonstrated the viability of using ^{210}Pb and ^{7}Be to age date the suspended sediment in various locations within Galveston Bay, but data can only be taken with little context in terms of the bigger picture of sediment transport throughout the bay. Additionally, TSS data shows that cold fronts accompanied with strong wind speed and a northern wind are important mechanisms for resuspending/remobilizing sediment in shallow estuaries. Ebb tide may also have a greater effect in resuspending sediment from the reduction of water levels within the bay. With Galveston bay being fairly shallow, the reduction of water levels from tide can have a large impact on sediment resuspension that occurs during cold fronts.

This study allows for a more thorough understanding of the sediment transport and trapping within the bay along with the particle/pollutant residence times. Particle movement is often back and forth due to the small tidal patterns and low flushing rate characteristic to Galveston Bay allowing them to disperse over the entirety of the bay (Du et al., 2020). Therefore, pollutant particles that adsorb to suspended sediment may spend months in the bay potentially degrading the water quality and overall ecosystem health. Cold front events accompanied with high amount of rainfall and strong winds can assist in larger quantity of upper/mid bay water transport out of the bay.

6. FUTURE PLANS

In order to further validate the method created by Matisoff et al. (2005), more samples at both sites need to be collected. Also, adding more sites within the middle bay would create a more thorough understanding of suspended sediment in Galveston Bay. Being able to collect more samples during the main cold front occurrences (October-March) and tropical storms/hurricanes will complete the study. Sample collection of the seabed before each cold front may allow for a greater understanding of whether suspended sediment has a greater input of previously deposited sediment or not. The ability to measure TSS concentrations and isotope ratios from the collection of these samples during cold fronts and tropical storms/hurricanes allows for a more complete understanding of sediment remobilization during both types of meteorological events.

REFERENCES

Baskaran, M., Coleman, C. H., & Santschi, P. H. (1993). Atmospheric depositional fluxes of 7Be and 210Pb at Galveston and College Station, Texas. *Journal of Geophysical Research: Atmospheres*, *98*(D11), 20555-20571.

Baskaran, M., & Santschi, P. H. (1993). The role of particles and colloids in the transport of radionuclides in coastal environments of Texas. *Marine Chemistry*, *43*(1-4), 95-114.

Baskaran, M., & Swarzenski, P. (2007). Seasonal variations on the residence times and partitioning of short-lived radionuclides (234Th, 7Be and 210Pb) and depositional fluxes of 7Be and 210Pb in Tampa Bay, Florida. *Marine Chemistry*, *104*(1-2), 27-42.

Biggs, R. B. (1970). Sources and distribution of suspended sediment in northern Chesapeake Bay. *Marine Geology*, *9*(3), 187-201.

Booth, J. G., Miller, R. L., McKee, B. A., & Leathers, R. A. (2000). Wind-induced bottom sediment resuspension in a microtidal coastal environment. *Continental Shelf Research*, *20*(7), 785-806.

Brost, R. A., Feichter, J., & Heimann, M. (1991). Three-dimensional simulation of 7Be in a global climate model. *Journal of Geophysical Research: Atmospheres*, *96*(D12), 22423 22445.

Byrne, J.R., 1975. Holocene depositional history of Lavaca Bay, Central Texas Gulf Coast. Dissertation, University of Texas, Austin, TX.

Carlin, J., Lee, G., Dellapenna, T., & Laverty, P. (2016). Sediment resuspension by wind, waves, and currents during meteorological frontal passages in a micro-tidal lagoon. *Estuarine, Coastal and Shelf Science*, *172*, 24-33.

Center for Sustainability and the Global Environment [SAGE], 2002. Global River Discharge Database. Center for Sustainability and the Global Environment, Gaylord Nelson Institute for Environmental Studies. University of Wisconsin-Madison. Online dataset, entry 2649, http:// www.sage.wisc.edu/riverdata/.

Chambers, M., Mitchell, A., Fine, A., Mulder, K., Rainville, L., Hackett, D., ... & Tujague, A. (2018). Port Performance Freight Statistics Program: Annual Report to Congress 2017.

Chao, J. Y., Zhang, Y. M., Kong, M., Zhuang, W., Wang, L. M., Shao, K. Q., & Gao, G. (2017). Long-term moderate wind induced sediment resuspension meeting phosphorus demand of phytoplankton in the large shallow eutrophic Lake Taihu. *PloS one*, *12*(3), e0173477.

Cox, D. T., Tissot, P., & Michaud, P. (2002). Water level observations and short-term predictions including meteorological events for entrance of Galveston Bay, Texas. *Journal of waterway, port, coastal, and ocean engineering*, *128*(1), 21-29.

Dellapenna, T., Allison, M., Gill, G., Lehman, R., & Warnken, K. (2006). The impact of shrimp trawling and associated sediment resuspension in mud dominated, shallow estuaries. *Estuarine, Coastal and Shelf Science*, *69*(3-4), 519-530.

Dellapenna, T. M., Hoelscher, C., Hill, L., Al Mukaimi, M. E., & Knap, A. (2020). How tropical cyclone flooding caused erosion and dispersal of mercury-contaminated sediment in an urban estuary: The impact of Hurricane Harvey on Buffalo Bayou and the San Jacinto Estuary, Galveston Bay, USA. *Science of The Total Environment*, *748*, 141226.

Du, J., Park, K., Dellapenna, T. M., & Clay, J. M. (2019). Dramatic hydrodynamic and sedimentary responses in Galveston Bay and adjacent inner shelf to Hurricane Harvey. *Science of the Total Environment*, *653*, 554-564.

Du, J., & Park, K. (2019). Estuarine salinity recovery from an extreme precipitation event: Hurricane Harvey in Galveston Bay. *Science of the total environment*, *670*, 1049-1059.

Du, J., Park, K., Yu, X., Zhang, Y.J. and Ye, F., (2020). Massive pollutants released to Galveston Bay during Hurricane Harvey: Understanding their retention and pathway using Lagrangian numerical simulations. *Science of The Total Environment*, *704*: 135364.

Guo, M., Li, X., Song, C., Liu, G., & Zhou, Y. (2020). Photo-induced phosphate release during sediment resuspension in shallow lakes: A potential positive feedback mechanism of eutrophication. *Environmental Pollution*, *258*, 113679.

Evrard, O., Laceby, J., Huon, S., Lefèvre, I., Sengtaheuanghoung, O., & Ribolzi, O. (2016). Combining multiple fallout radionuclides (137Cs, 7Be, 210Pbxs) to investigate temporal sediment source dynamics in tropical, ephemeral riverine systems. *Journal of Soils and Sediments*, *16*(3), 1130-1144.

Ha, H., & Park, K. (2012). High-resolution comparison of sediment dynamics under different forcing conditions in the bottom boundary layer of a shallow, micro-tidal estuary. *Journal of Geophysical Research: Oceans*, *117*(6).

Haby, M. G., Miget, R. J., & Falconer, L. L. (2009). Hurricane damage sustained by the oyster industry and the oyster reefs across the Galveston Bay system with recovery recommendations. *A Texas AgriLife Extension Service/Sea Grant Extension Program Staff Paper*.

Hardenbergh, W. A. (1938). *Water Supply and Purification*. International textbook Company.

Hardy, J. W., & Henderson, K. G. (2003). Cold front variability in the southern United States and the influence of atmospheric teleconnection patterns. *Physical geography*, *24*(2),120 137.

Herdendorf, C., Klarer, D. M., & Herdendorf, R. C. (2004). *The Ecology of Old Woman Creek, Ohio: An Esturine and Watershed Profile*. Ohio Department of Natural Resources.

Henry, W. K. (1979). Some aspects of the fate of cold fronts in the Gulf of Mexico. *Monthly Weather Review*, *107*(8), 1078-1082.

Hossain, S., Eyre, B., & McConchie, D. (2001). Suspended sediment transport dynamics in the sub-tropical micro-tidal Richmond River estuary, Australia. *Estuarine, Coastal and Shelf Science*, *52*(5), 529-541.

Huang, D., Du, J., & Zhang, J. (2011). Particle dynamics of 7Be, 210Pb and the implications of sedimentation of heavy metals in the Wenjiao/Wenchang and Wanquan River estuaries, Hainan, China. *Estuarine, Coastal and ShelfScience*, *93*(4), 431-437.

Kemp, G. P. (1986). Mud Deposition at the Shoreface: Wave and Sediment Dynamics on the Chenier Plain of Louisiana. Ph.D. Dissertation, Louisiana State University, 146p.

Kuehl, S. A., Miller, E. J., Marshall, N. R., & Dellapenna, T. M. (2017). Recent paleoseismicity record in Prince William Sound, Alaska, USA. *Geo-Marine Letters*, *37*(6), 527-536.

Lin P., Guo L., Chen M., Cai Y., (2013). Distribution, partitioning and mixing behavior of phosphorus species in the Jiulong River estuary. *Marine Chemistry* 157, 93 105.

Mabit, L., & Blake, W. (2019). *Assessing Recent Soil Erosion Rates through the Use of Beryllium-7 (Be-7)* (p. 69). Springer Nature.

MacIntyre, H. L., & Cullen, J. J. (1996). Primary production by suspended and benthic microalgae in a turbid estuary: time-scales of variability in San Antonio Bay, Texas. *Marine Ecology Progress Series*, *145*, 245-268

Matisoff, G., Wilson, C., & Whiting, P. (2005). The 7Be/210PbXS ratio as an indicator of suspended sediment age or fraction new sediment in suspension. *Earth Surface Processes and Landforms*, *30*(9), 1191-1201.

Matos, T., Faria, C. L., Martins, M. S., Henriques, R., Gomes, P. A., & Goncalves, L. M. (2019). Development of a cost-effective optical sensor for continuous monitoring of turbidity and suspended particulate matter in marine environment. *Sensors*, *19*(20), 4439.

Minella, J. P., Merten, G. H., Reichert, J. M., & Clarke, R. T. (2008). Estimating suspended sediment concentrations from turbidity measurements and the calibration problem. *Hydrological Processes: An International Journal*, *22*(12), 1819-1830.

Moeller, C. C., Huh, O. K., Roberts, H. H., Gumley, L. E., & Menzel, W. P. (1993). Response of Louisiana coastal environments to a cold front passage. *Journal of Coastal Research*, 434-447.

Morse, J. W., Presley, B. J., Taylor, R. J., Benoit, G., & Santschi, P. (1993). Trace metal chemistry of Galveston Bay: water, sediments and biota. *Marine Environmental Research*, *36*(1), 1-37.

Novoveská, L., & MacIntyre, H. L. (2019). Study of the seasonality and hydrology as drivers of phytoplankton abundance and composition in a shallow estuary, Weeks Bay, Alabama (USA). *J Aquac Mar Biol*, *8*(3), 69-80.

Olsen, C., Larsen, I., Lowry, P., Cutshall, N., & Nichols, M. (1986). Geochemistry and deposition of 7Be in river-estuarine and coastal waters. *Journal of Geophysical Research*, *91*(Cl), 896-908.

Olsen, C. R., Larsen, I. L., Lowry, P. D., Cutshall, N. H., Todd, J. F., Wong, G. T. F., & Casey, W. H. (1985). Atmospheric fluxes and marsh-soil inventories of 7Be and 210Pb. *Journal of Geophysical Research: Atmospheres*, *90*(D6), 10487-10495.

Olsen, C. R., Thein, M., Larsen, I. L., Lowry, P. D., Mulholland, P. J., Cutshall, N. H., ... & Windom, H. L. (1989). Plutonium, lead-210, and carbon isotopes in the Savannah estuary: riverborne versus marine sources. *Environmental science & technology*, *23*(12), 1475-1481.

Pepper, D. A., Stone, G. W., & Wang, P. (1999). Bottom boundary layer parameters and sediment transport on the Louisiana inner-shelf during cold front passages. *Gulf Coast Association of Geological Societies Transactions*, 49, 432-439.

Perez, B., Day, J., Rouse, L., Shaw, R., & Wang, M. (2000). Influence of Atchafalaya River discharge and winter frontal passage on suspended sediment concentration and flux in Fourleague Bay, Louisiana. *Estuarine, Coastal and Shelf Science*, *50*(2), 271-290.

Roberts, H., Huh, O., Hsu, S., Rouse, L., Rickman, D., (1987). Impact of cold-front passages on geomorphic evolution and sediment dynamics of the complex Louisiana coast, Coastal Sediments '87. ASCE 1950-1963.

Saari, H., Schmidt, S., Castaing, P., Blanc, G., Sautour, B., Masson, O., & Cochran, J. (2010). The particulate 7Be/210Pbxs and 234Th/210Pbxs activity ratios as tracers for tidal-to-seasonal particle dynamics in the Gironde estuary (France): Implications for the budget of particle-associated contaminants. *Science of the Total Environment*, *408*(20), 4784-4794.

Sanford, L. P., & Halka, J. P. (1993). Assessing the paradigm of mutually exclusive erosion and deposition of mud, with examples from middle Chesapeake Bay. *Marine Geology*, *114*(12), 37 57.

Santschi, P. H., Presley, B. J., Wade, T. L., Garcia-Romero, B., & Baskaran, M. (2001). Historical contamination of PAHs, PCBs, DDTs, and heavy metals in Mississippi river Delta, Galveston bay and Tampa bay sediment cores. *Marine EnvironmentalResearch*, *52*(1), 51-79.

Sidik, M. B. J., Gohin, F., Bowers, D., Howarth, J., & Hull, T. (2017). The relationship between Suspended Particulate Matter and Turbidity at a mooring station in a coastal environment: consequences for satellite-derived products.

Solis, R. S., & Powell, G. (1999). Hydrography, residence times, and physical processes. *Biogeochemistry of Gulf of Mexico Estuaries. New York: John Wiley*, 29-61.

Sommerfield, C. K., Nittrouer, C. A., & Alexander, C. R. (1999). 7Be as a tracer of flood sedimentation on the northern California continental margin. *Continental Shelf Research*, *19*(3), 335-361.

Stunz, G. W., Minello, T. J., & Rozas, L. P. (2010). Relative value of oyster reef as habitat for estuarine nekton in Galveston Bay, Texas. *Marine Ecology Progress Series*, 406, 147 159.

Taylor, A., Blake, W. H., Smith, H. G., Mabit, L., & Keith-Roach, M. J. (2013). Assumptions\and challenges in the use of fallout beryllium-7 as a soil and sediment tracer in river basins. *Earth science reviews*, *126*, 85-95.

United States Geological Survey [USGS], 2005. US Geological Survey suspended-sediment database, daily values of suspended sediment and ancillary data. An on-line database: http://co.water.usgs.gov/sediment/.

Vousdoukas, M., Aleksiadis, S., Grenz, C., & Verney, R. (2011). Comparisons of acoustic and optical sensors for suspended sediment concentration measurements under non-homogeneous solutions. *Journal of Coastal Research*, 160-164. Retrieved May 18, 2021, from https://www.jstor.org/stable/26482153

Walker, N. D., & Hammack, A. B. (2000). Impacts of winter storms on circulation and sediment transport: Atchafalaya-Vermilion Bay region, Louisiana, USA. *Journal of Coastal Research*, 996-1010.

Wang, Z., Yang, W., Chen, M., Lin, P., & Qiu, Y. (2013). Intra-annual deposition of atmospheric 210Pb, 210Po and the residence times of aerosol in Xiamen, China. *Aerosol and Air Quality Research*, *14*(5), 1402-1410.

Webster, T., & Lemckert, C. (2002). Sediment resuspension within a microtidal estuary/embayment and the implication to channel management. *Journal of Coastal\Research*, (36), 753-759.

Williams, J.R., Kuehl, S.A., Clyne, E.R. and Dellapenna, T.M., 2018. Seasonal variability of 7Be in suspended sediments from the Copper River, Alaska: implications for quantifying recent flood deposits in coastal environments. Geo Marine Letters, 38(6), pp.467-480.

Winterwerp, J. C., & Van Kesteren, W. G. (2004). *Introduction to the physics of cohesive sediment dynamics in the marine environment*. Elsevier.